第88卷 第12期
2014年12月 地 质 学 报 ACTA GEOLOGICA SINICA Vol. 88 No. 12
Dec. 2014

斑岩铜矿床的基本特征和研究勘查新进展

毛景文[1)]，罗茂澄[2)]，谢桂青[1)]，刘军[1)]，吴胜华[1)]
1）中国地质科学院矿产资源研究所，国土资源部成矿作用与资源评价重点实验室，北京，100037；
2）中国地质大学地球科学与资源学院，北京，100081

内容提要：斑岩铜矿是铜资源的主要供给矿种，长期以来是研究和勘查的重要目标。2000年以来进入了新一轮高潮，找矿勘查取得了新突破，研究获得重大进展。迄今为止，已探明斑岩铜矿储量约18×10^8t，主要分布在南美和北美西部大陆边缘、西南太平洋岛弧、中亚地区以及特提斯东欧段、伊朗—巴基斯坦段和我国西藏地区，其中南美西部大陆边缘储量达11×10^8t。已探明储量按时代分布，从新生代、中生代、晚古生代、早古生代到前寒武纪，依次降低。斑岩铜矿通常出现在大洋俯冲带上部，在岛弧形成斑岩铜金矿，在大陆边缘形成斑岩铜钼矿或斑岩铜金钼矿。俯冲板片由陡倾角变为缓倾角，甚至平板，有利于成矿；超大型矿床在空间上往往与无震海岭、海口山连和海中高原的低角度俯冲有关，大洋板片广泛发育的转换断层易于被海水交代，当俯冲到大陆或岛弧之下，有利于形成含矿岩浆；而在大陆不同构造单元的结合部位，俯冲板片易于撕裂，也是成矿带形成的重要场所。由于板片俯冲，将大量海水及海底沉积物（包括硫酸盐）携带进入软流圈，俯冲板片脱水导致交代作用和软流圈地幔楔的部分熔融被认为是弧岩浆成因的主要过程。这种高氧化度和富含挥发组分的基型岩浆在下地壳经历了MASH过程和分异演化，逐渐形成中酸性含矿岩浆，这种岩浆比重较轻，沿断裂带上升到浅表定位和成矿。过去10多年对于大陆斑岩铜矿的研究越来越受到关注，目前关注的焦点是成矿物质来自于大陆内部的壳幔反应产物（包括新生下地壳）还是俯冲板片残留重熔形成的交代岩石圈。从找矿勘查角度，矿床模型研究依然是重点，从单个典型矿化蚀变模型到矿床组合模型。此外，近年针对斑岩铜矿系统中的蚀变矿物（例如，绿泥石、绿帘石、明矾石和粘土矿物等），开展Footprint（找矿印痕）研究，探讨矿体的分布规律，提出找矿标志。

关键词：斑岩铜矿；俯冲与成矿；大陆成矿；时空分布规律；矿床模型

过去30～40年，斑岩铜矿床一直是找矿勘查和科学技术研究的重要目标，而且长盛不衰。在20世纪70～80年代曾出现过一个高峰期，过去10年以来又迎来一个新的高峰期。在过去10年的国际矿床会议中，斑岩铜矿研究与勘查进展凸显一枝独秀，无论是在成矿理论和找矿效果方面都取得了重要进展。对此，姚春亮等（2007）、杨志明和侯增谦（2009）和陈华勇和肖兵（2014）曾经进行过比较全面地综述。本文基于前人工作基础，结合最近几年的新进展，在此针对一些找矿勘查和研究的新进展，进行总结研究。

1 斑岩铜矿时空分布特点

大多数斑岩铜矿床出现于显生宙，仅极少数形成于前寒武纪，例如，我国中条山地区的铜矿峪中元古代斑岩铜矿（王植和闻广，1957），加拿大西北安大略省Parmour太古宙斑岩铜矿（Davies and Luhta，1978）和魁北克东北部太古宙Lac Troilus斑岩铜金矿（Fraser，1993），印度的Malajkhand（Sikka and Nehru，1997）和澳大利亚的Boddington元古代斑岩铜矿。绝大多数显生宙斑岩铜矿分布于环太平洋、古亚洲造山带和新特提斯造山带，成矿时代分别主要为中新生代、晚古生代和新生代。无论是前寒武纪还是显生宙，斑岩铜矿广泛形成于板块聚合边界（Sillitoe，2010）。

在图1中Sillitoe（2013）标注出重要矿带及超大型斑岩铜矿的空间分布及其已探明的储量。考虑到我国勘查进展，在其中补充了我国冈底斯，班公湖—怒江、长江中下游成矿带及德兴和驱龙超大型矿床。此外，也补充了新特提斯成矿带部分资料。

注：本文由中国地质调查局资助项目（编号12120113093600）的部分成果。
收稿日期：2014-10-20；改回日期：2014-11-15；责任编辑：郝梓国，周健，黄敏。
作者简介：毛景文，男，1956年生。研究员。从事矿床学与地球化学研究。通讯地址：北京市西城区百万庄大街26号，100037；Email：jingwenmao@263.net。

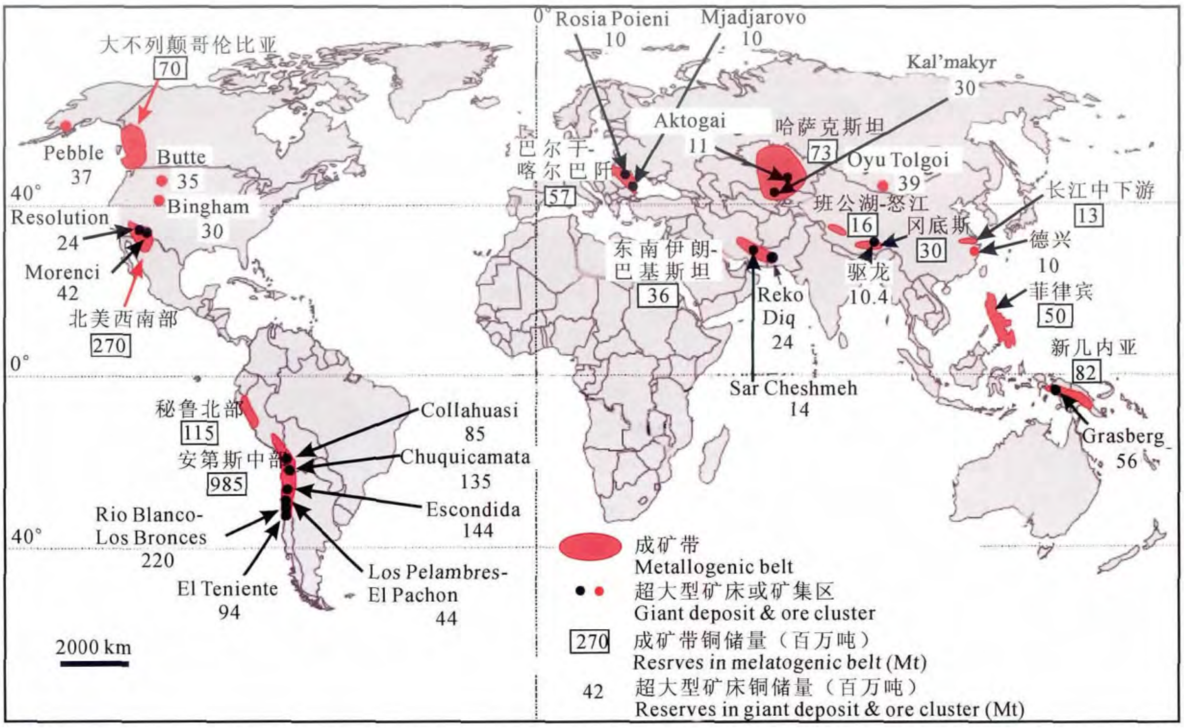

图 1 全球斑岩铜矿主要成矿带、大型矿集区及超大型矿床分布图(据 Sillitoe，2013；Yakubchuk，2012；Richards et al.，2012 **修改，并增加中国和特提斯西段成矿带、矿集区及超大型矿床**)

Fig. 1 The distribution of global metallogenic belts and clusters of porphyry Cu deposits as well as giant porphyry Cu deposits (modified from Sillitoe，2013；Yakubchuk，2012；Richards et al.，2012)

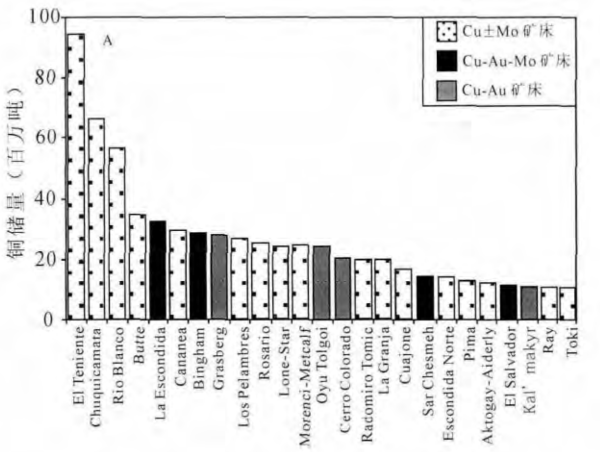

图 2 全球 25 个超大型斑岩铜矿储量分布图

(**据** Cooke et al.，2005)

Fig. 2 The 25 largest porphyry copper deposits，based on the tonnage of contained copper metal (after Cooke et al.，2005)

从分布图(图 1)上可以看出，斑岩铜矿在空间上分布具有明显的不均一性，通常在某些特殊空间发生巨量聚集。Cooke **等**(2005)**对全球** 25 **个最大斑岩铜矿进行了时代和储量统计(图** 2)，**发现大多数超大型矿床均形成于新生代，主要分布于南美安第斯山中部、北美科迪勒拉山西南部和西北部、阿拉斯加、西南太平洋岛弧和特提斯成矿域的伊朗等地。在古亚洲成矿带中的** Oyu Tolgoi **形成于早古生代，时代为** 411 Ma (Ivanhoe Mines，2004)，**哈萨克斯坦的** Aktogai **和乌兹别克斯坦的** Kal'makyr **形成于晚古生代，时代为** 320～330 Ma(Chen et al.，2014)。**从图** 1 **和图** 2 **中可以看出，前两者提供的某些矿床储量数据不一致，除了来源和年代差异外，导致这种结果的主要原因是** Cooke **等** (2005)**提供的是单个矿床的储量数字，而** Sillitoe (2013)**使用的是矿集区储量数字。值得指出的是美国阿拉斯加州的** Pebble **斑岩铜金矿和蒙古国的** Oyu Tolgoi **斑岩铜金矿是** 2000 **年以来全球最重要的发现。由于** Pebble **斑岩铜金矿探明时间较晚**(Lang et al.，2013)，**在图** 2 **中未列入。**

美洲大陆西部边缘拥有 20 **多个超大型斑岩型铜钼矿和铜金矿，包括智利中部** El Teniente，Chuquicamata **和** Río Blanco-Los Bronces **三个世界最大的斑岩铜矿，安第斯中部和北美科迪勒拉西南部是全球第一和第二斑岩铜矿富集区，后者也是当**

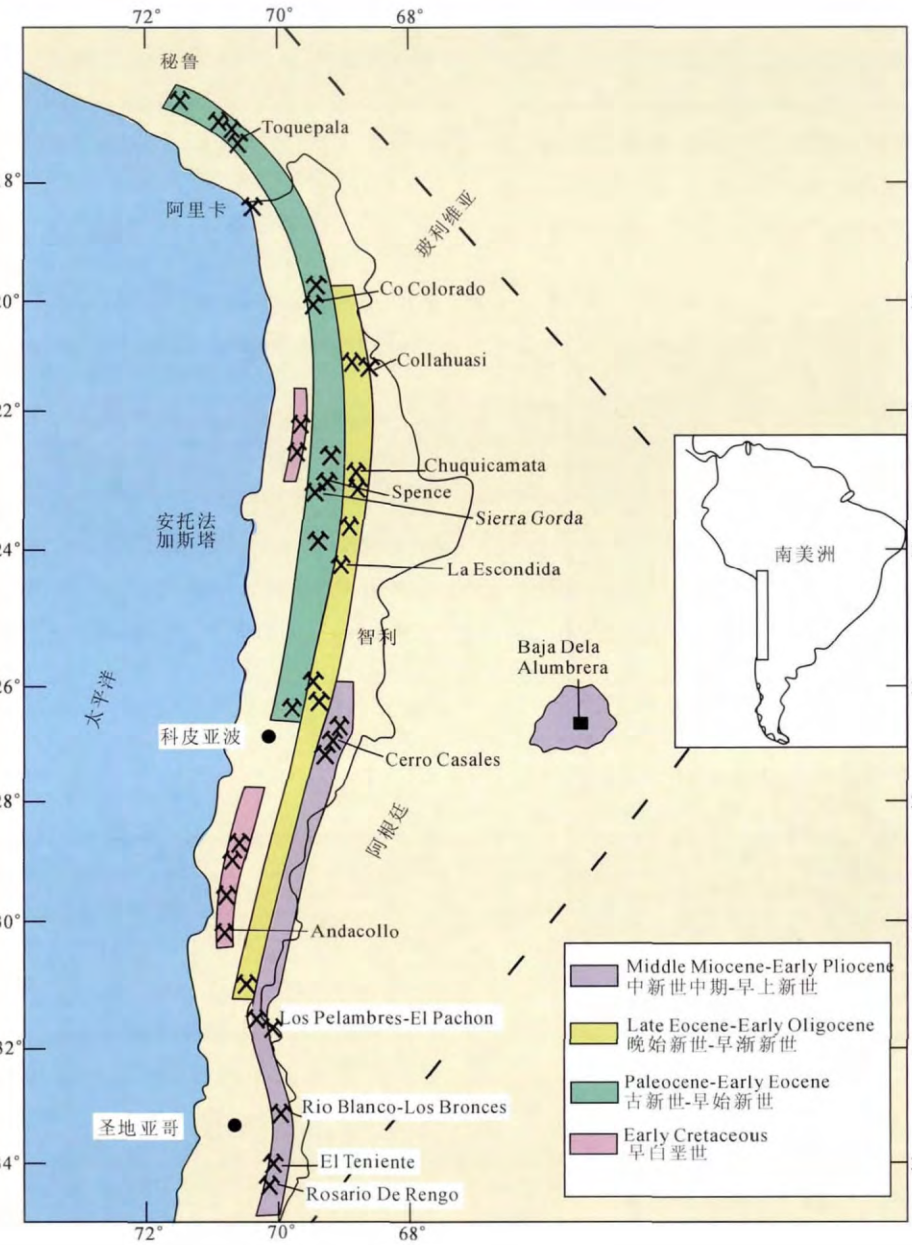

图 3 智利中北部斑岩铜矿时空分布图(据 Dekart et al.，2014)

Fig. 3 Metallogenic belts in central-northern Chile (after Dekart et al.，2014)

代斑岩铜矿成矿理论最早发祥地(Leveille and Stegen，2012)。**在南美大陆边缘中部智利—秘鲁—阿根廷西北部，铜矿在空间上从西部滨海向东陆内呈** 4 **个南北走向带的分布，分别为白垩纪氧化铁铜金矿**(IOCG)、**古新世—早始新世**(66～52 Ma)**斑岩铜矿、晚始新世—早渐新世**(42～31 Ma)**斑岩铜矿和中新世中期—早上新世**(16～5 Ma)**斑岩铜矿**(**图** 3)(Deckart et al.，2014)。**而在北美科迪勒拉西南部，斑岩铜矿发育于晚白垩纪—早新生代**(75～45Ma)，**呈分散矿集区形式出现于大陆内部**(Leveille and Stegen，2012；Barra and Valencia，2014)，**主要集中在美国的亚利桑那州、新墨西哥州、犹他州和德克萨斯州以及墨西哥北部，从大陆边缘，向陆内延伸** 1500 **多公里。与太平洋东部大陆边缘相反，在太平洋西部大陆边缘没有发现世界级大型斑岩铜矿床，仅德兴矿田的铜储量大于** 1000 **万吨。而且已探明的绝大多数斑岩铜矿发育于我国东部大陆边缘，集中发育于钦杭、长江中下游和北太行山-大兴安岭东侧三个北东走向的线性成矿带中以及大陆边缘一系列伸展盆地中，前三个成矿带形成于挤压环境**(170～137Ma)，**后者形成于伸展环境**(110～80 Ma)(**图** 4)(Mao et al.，2011a，2011b，2013，

2014)。西南太平洋岛弧是全球第三大斑岩铜矿富集区,拥有巴布亚新几内亚 Grasberg 铜金矿以及印度尼西亚 Batu Hijau, Tampakan, Atlas 和 Sipilay 超大型斑岩型金铜矿,这些是大洋岛弧斑岩铜矿的代表,明显特点是均为斑岩铜矿富金,更多表现为富铜的斑岩型金矿(Pollard et al., 2005; Hollings et al., 2013)。

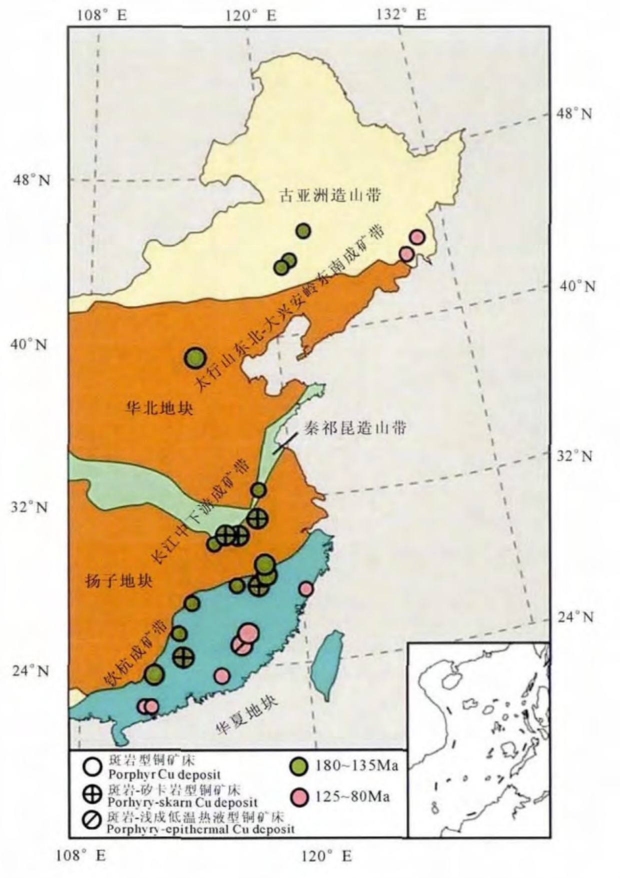

图 4　中国东部中生代斑岩(矽卡岩型)铜矿分布图
(据 Mao et al., 2014 修改)

Fig. 4　Distribution of major porphyry copper deposits in East China (modified from Mao et al., 2014)

古亚洲成矿域是全球第四大斑岩铜矿富集区带,拥有蒙古 Oyu Tolgoi,哈萨克斯坦 Aktogai 和乌兹别克斯坦 Kal'makyr 超大型矿床。该富集区特点是成矿时代跨度很大,从早古生代早期到中生代中晚期(Yakubchuk et al., 2012;Seltmann et al., 2014;Chen et al., 2014)。在古亚洲成矿域中,斑岩铜矿分布特点为从北部和南部向中部成矿时代变新(即:向中奥陶世—泥盆纪逐渐到晚石炭世),从东到西也是具有同样趋势(即从晚泥盆世到晚石炭世),而有关的斑岩钼矿则从西向东,成矿时代从晚石炭世—早二叠世变为三叠纪(图 5)(Mao et al., 2014)。这些可能表明了古亚洲洋的多地块多次增生及大洋闭合和碰撞后演化特征(图 6),即在岛弧环境形成斑岩 Cu-Au 矿及斑岩 Cu-Mo 矿(辉钼矿高度富 Re/Os),在活动大陆边缘形成斑岩 Cu-Mo 矿和后碰撞型多种类型金属矿产。位于古亚洲东北部的蒙古-鄂霍茨克洋曾是古太平洋的组成部分,自三叠纪中期从西向东逐渐闭合,形成了一套三叠纪至中晚侏罗世(240～160 Ma)的斑岩铜矿带(Yakubchuk et al., 2012; Mao et al., 2014)(图 5)。

新特提斯斑岩铜矿带长达 10000 多公里,东起始于缅甸,经越南北部、我国红河-哀牢山和西藏、阿富汗、巴基斯坦、伊朗、小高加索、土耳其,延伸到东欧巴尔干半岛-喀尔巴阡地区,尤其是在东欧的巴尔干-喀尔巴阡地区和伊朗-阿富汗-巴基斯坦地区形成一系列大型-超大型矿床,包括伊朗的 Sar Cheshmeh,巴基斯坦的 Reko Diq,罗马尼亚的 Rosia Poieni 和塞尔维亚的 Majdan Pek(Cooke et al., 2005)。巴尔干-喀尔巴阡地区的斑岩铜矿形成于晚白垩世(90～65 Ma),成因上与钙碱性-高钾钙碱性火山-侵入岩有关,被认为是多阶段俯冲的产物(Ciobanu et al., 2002; Heinrich and Neubauer, 2002)。伊朗-阿富汗-巴基斯坦地区斑岩铜矿形成时代为 35～6 Ma,并且从西北向东南年龄渐次变新,其成矿与阿拉伯半岛与欧亚大陆聚合过程有密切的关系,两个陆块最终碰撞时间在中新世,尽管阿曼海湾仍在俯冲闭合之中(Hezarkhani,2006;Chiu et al., 2013;Mahdavi et al., 2015)。过去 10 年,在我国冈底斯和班公湖-怒江斑岩铜矿找矿取得了重要进展,发现了一批大型矿床(Hou et al., 2009; Qin, 2011),包括 1040 万吨的驱龙斑岩铜钼矿(郑有业等,2004;杨志明等,2008)和甲玛斑岩铜钼矿(唐菊兴等,2011)。冈底斯斑岩铜矿的成矿时代为中晚侏罗世和中新世(Tafti et al., 2009; 芮宗瑶等,2003;Hou et al., 2003),而班公湖-怒江的成矿时代为白垩纪,可能形成于岛弧环境(Li et al., 2011; Sun et al., 2014)。基于前人的大量工作,Mao 等(2014)总结提出冈底斯成矿带斑岩铜矿和斑岩钼矿从俯冲到碰撞后的三阶段成矿模型(图 7)。在欧亚交界处的土耳其具有很好的找矿前景,是目前全球找矿勘查新的重要目标区之一(Yigit, 2009)。

2　俯冲环境斑岩铜矿

成矿环境:Sillitoe (1972)首先注意到斑岩铜矿

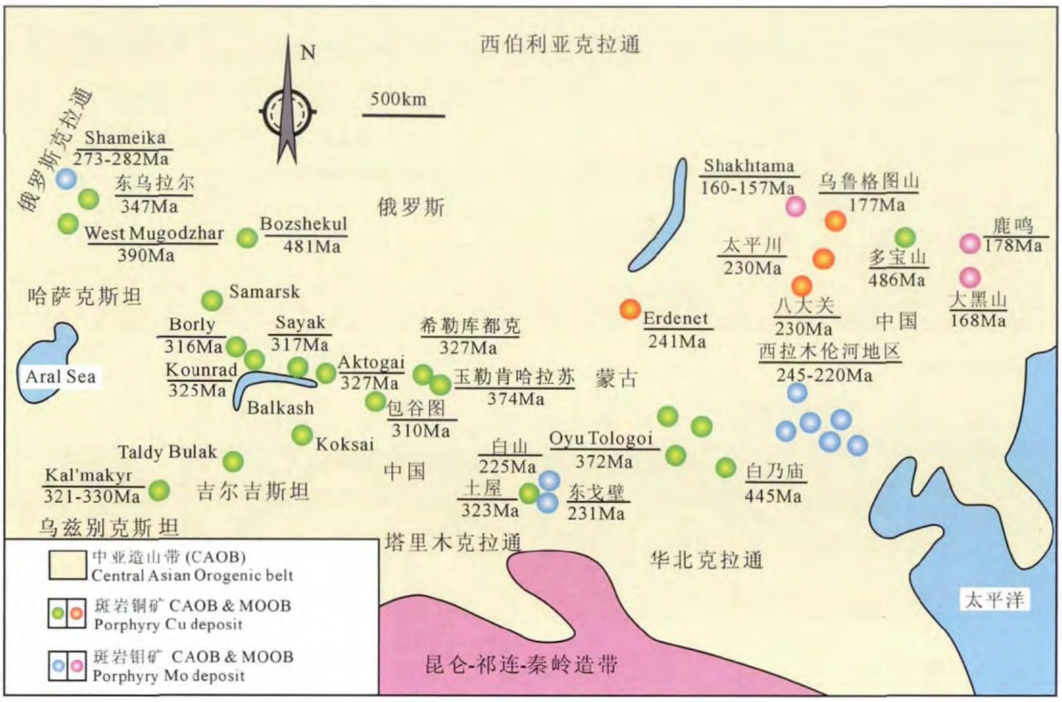

图 5　古亚洲(CAOB)及蒙古-鄂霍茨克(MOOB)造山带中斑岩铜矿和斑岩钼矿时空分布图

(据 Seltmann et al.,2005,2014;Mao et al.,2014;Chen et al.,2014;Yakubchuk et al.,2012 修改)

Fig. 5　Map showing distribution of major porphyry copper and porphyry molybdenum deposits in the Central Asian Orogenic Belt (CAOB) and Mongolia-Okhotsk Orogenic Belt (MOOB) (complied based on the diagrams and data of Seltmann et al., 2005, 2014; Mao et al., 2014; Chen et al., 2014; Yakubchuk et al., 2012)

与板块俯冲的关系,并提出俯冲板片环境中的构造成矿模式,认为与斑岩铜矿成矿有关的岩体是洋壳在俯冲过程中部分熔融的产物。Sillitoe (1998) 进一步研究认为斑岩铜矿形成于挤压环境,并注意到挤压导致地壳加厚与智利中北部、亚利桑那西南部、伊朗 Jaya 等超大型矿床形成上具有同步性,表明了挤压环境有利于形成斑岩铜矿。同时,注意到南美古新世—始新世弧于挤压走滑环境导致形成 Cujaone 超大型和 Toquepala 巨型矿床,而一些小型矿床出现在相邻的智利北部的引张环境(Sillitoe 1998)。Sillitoe (1998)总结提出挤压环境可有效地阻止岩浆直接穿过上地壳形成火山岩,因此形成比伸展环境更大的浅部岩浆房;挤压环境的浅部岩浆房很难喷发,从而促进了岩浆房的结晶分异,进而导致了挥发分的饱和以及大规模岩浆热液的形成;挤压环境下很难发育陡立的张性断裂,从而有效地限制了在岩浆房顶部形成岩株(枝)的数量,有利于岩浆热液的聚集。基于在秘鲁南部-智利北部古新世-渐新世岩石的研究,James 和 Sacks(1999)总结提出斑岩铜矿形成与大洋板片俯冲角度从正常到平板和再到正常有关,该过程具有 7 个特点:①一个宽广的碱性岩浆减少带;②由于挤压平面缩短;③平板板片上部岩石圈脱水;④由于岩石圈对流冷却导致异常的低热流;⑤回到正常俯冲和热软流圈作用及脱水地幔,引起湿熔;⑥地幔熔体通过大陆岩石圈导致地壳的大量熔融;⑦岩石圈减薄及薄弱区有利于热流循环,导致地壳的强烈缩短和隆起。James 和 Sacks(1999)进一步提出相似的深部过程很可能出现于其他成矿省的低角度俯冲。Murphy (2001) 研究指出美国西南部斑岩铜矿与低角度板块俯冲有关,其证据是缺少火山岩、广泛发育陆内变形和厚皮构造。Cooke 等(2005)通过对全球 25 个巨型斑岩铜矿和斑岩金铜矿的研究,发现 7 个巨型斑岩铜矿中的 6 个和 13 个巨型斑岩铜金矿中的 9 个在空间上都与无震海岭、海口山连和海中高原的低角度俯冲有关,导致地壳增厚、快速隆起和折返。这些特殊部位的洋壳俯冲也可以很好地解释为什么在南美洲中部自白垩纪以来的多期次大规模形成斑岩铜矿。Mao 等(2013,2014)研究提出中国东部地区 170～135 Ma 期间受 Izanagi 板块或古太平洋板块斜向低角度俯冲,沿华夏地块与扬子地块之间的新元古代缝合带钦杭带、扬子克拉通与秦岭褶皱带之间结合

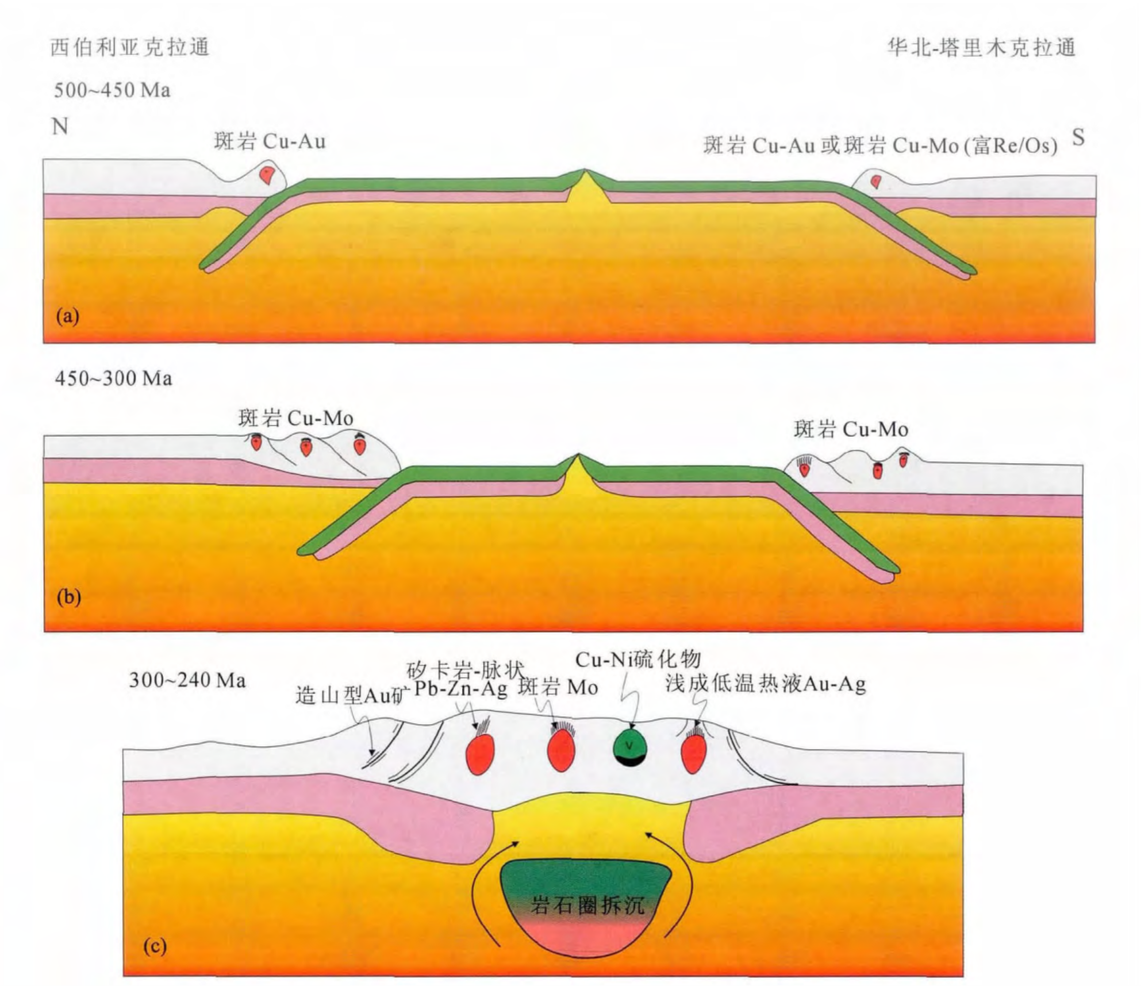

图 6 古亚洲洋增生与斑岩铜矿成矿作用的构造演化示意图

Fig. 6 The carton showing the tectonic accretions and related porphyry Cu metallogeny

带的长江中下游带以及大兴安岭—太行山东北段与东部平原结合带，俯冲板片撕裂和熔融导致生成含矿岩浆及上侵定位，形成 3 了个相互平行的北东向斑岩-矽卡岩型铜矿带(图 4)，之所以形成这 3 个矿带是由于俯冲板片在结合带发生撕裂和交代作用。前人(Uyeda and Miyashiro, 1974; Dickinson and Snyder, 1979; Thorkelson, 1996)曾注意到洋中脊俯冲与斑岩铜矿在空间上的关系，Sun 等(2010)对该方面研究进行了总结，提出大多数巨型斑岩铜矿与洋中脊俯冲有关。Ling 等 (2009)提出长江中下游地区斑岩-矽卡岩成矿带是洋中脊俯冲成矿的一个典型例子。最近，Richards 和 Holm (2013)研究发现大型-超大型斑岩铜矿与俯冲板片的转换断层具有成因联系。沿超基性洋壳或岩石圈内的转换断层通常发生交代作用(例如，蛇纹石化)，一旦俯冲到岛弧或大陆下，这些富水的岩石圈容易发生撕裂，导致地幔流上升和板片重熔，形成含矿熔浆。

岩浆来源：斑岩铜矿床在成因上主要与中酸性的钙碱性岩浆相关，其岩性介于石英闪长岩与花岗岩之间，其中，陆缘弧环境的含矿斑岩主要为钙碱性系列，少量为高钾钙碱性系列，岩性以花岗闪长岩和石英二长岩为主(Singer et al., 2005)；而岛弧环境的含矿斑岩通常为典型钙碱性系列，岩性以石英闪长岩为主，少数为花岗闪长岩、石英二长岩(Misra, 2000)；与斑岩铜钼矿有关的花岗质岩石主要为碱性花岗斑岩(Cooke et al., 2008)；斑岩铜金矿与碱性花岗岩有关(涂光炽，1998; Sillitoe et al., 1997; Mueller and Groves, 2000)。

对于在俯冲环境含矿岩浆来源和形成过程，前人已经进行了大量的探索，获得了丰硕的成果。以钙碱性岩浆为代表的含矿岩浆通常被认为是俯冲的大洋板片直接熔融的产物(Sillitoe, 1972, Burnham et al., 1979)，俯冲板片脱水导致交代作用和软流圈地幔楔的部分熔融被认为是弧岩浆成因的主要过

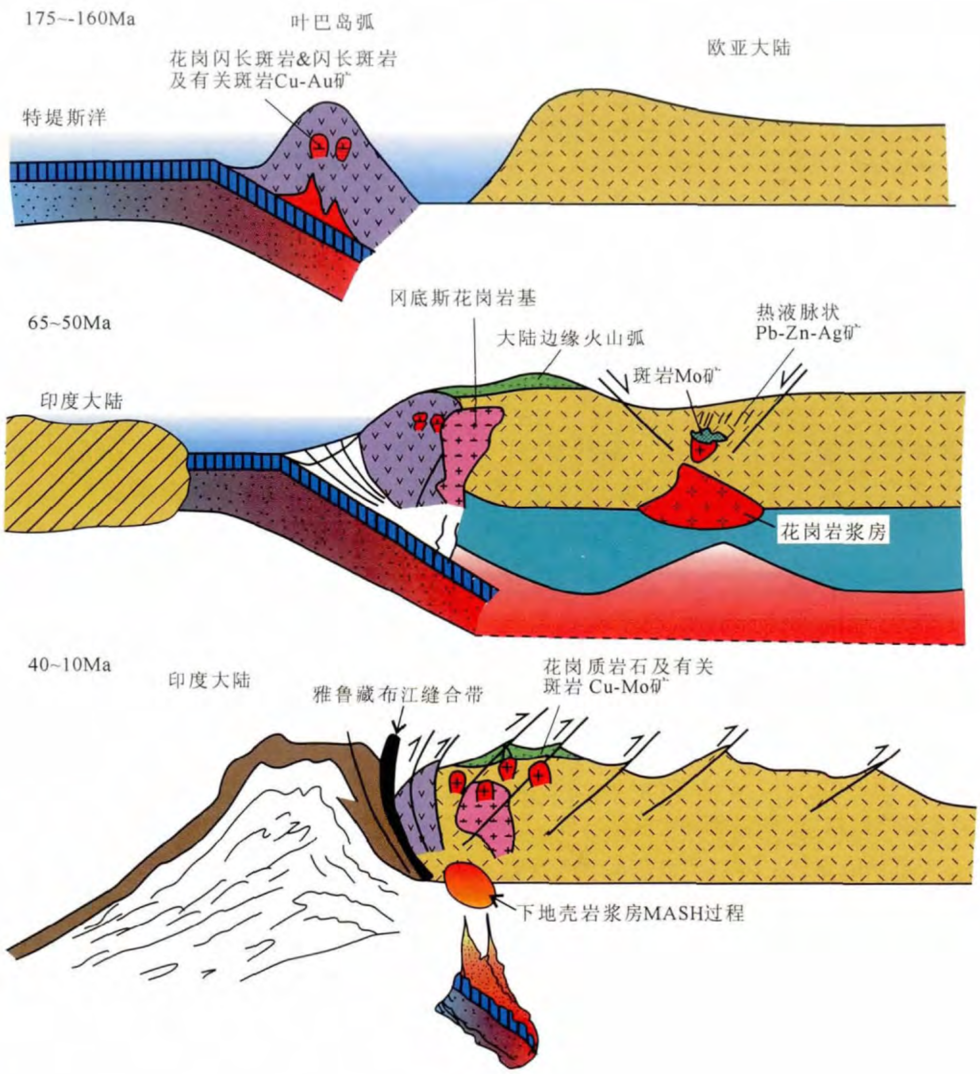

图 7　冈底斯斑岩铜矿带三阶段构造演化与成矿图

Fig. 7　Carton showing the tectonic evolution and metallogeny of porphyry copper and porphyry molybdenum deposits in the Gangdese ore belt

(a)—叶巴岛弧与中侏罗世板块俯冲有关的斑岩 Cu-Au 矿;(b)—俯冲末期-碰撞早期大陆边缘弧后盆地内中晚古新世—早始新世斑岩钼矿-脉状 Pb-Zn 矿;(c)—晚始新世—早中新世后碰撞多阶段伸展环境的斑岩 Cu-Mo 矿(据 Mao et al., 2014 修改)

(a)—Middle Jurassic subduction related porphyry Cu-Au deposits in the Yeba Island Arc; (b)—Late Paleocene-Early Eocene porphyry Mo and hydrothermal vein type Pb-Zn deposits related to late subduction and early collision in the back arc basin of the continental margin; (c)—Late Eocene-Early Miocene porphyry Cu-Mo (W) systems in multiple extensional settings within the post-collision stage (modified from Mao et al., 2014)

程(Tatsumi, 1986, 1989; Peacock, 1993; Schmidt and Poli, 1998; Bourdon et al., 2003; Grove et al., 2006, 2012). **脱水橄榄质软流圈的部分熔融产物是高镁玄武岩或苦橄岩**(DeBari and Sleep, 1991; Eggins, 1993; Thirlwall et al., 1996; Greene et al., 2006),**而且具有相当高的水含量(通常** 1%~7.5% H_2O; Sobolev and Chaussidon, 1996; Moore and Carmichael, 1998; Ulmer, 2001; Pichavant et al., 2002; Cervantes and Wallace, 2003; Grove et al., 2003, 2012; Wallace, 2005; Kelley et al., 2010; Zimmer et al., 2010). **它们比来自典型软流圈的熔体具有更高的氧化度,估计氧逸度**($\log fO_2$)**相对于铁橄榄石-磁铁矿-石英缓冲线**(ΔFMQ) **变化在**+1 ~ +3 **之间**(Ballhaus, 1993; Brandon and Draper, 1996; Parkinson and Arculus, 1999; de Hoog et al., 2004)。Sun **等**

(2014)指出在含矿岩浆中硫酸盐(SO_4^{2-})比硫化物(S^{2-})的溶解性大10倍,因此,硫的溶解度依赖于氧逸度。业已证明由于氧化度控制硫的溶解性和硫的种类以及亲硫和亲石元素的溶解度和配分,从成熟的俯冲带到达上部板块岩浆通常是相对氧化状态较高(Jugo et al., 2005, 2010; Klimm et al., 2012)。随着氧化状态增高到最大值 $\Delta FMQ \approx 1 \sim 2$ (Brandon et al., 1996; Parkinson and Arculus, 1999; Jenner et al., 2010; Botcharnikov et al., 2011; Jégo and Pichavant, 2012)以硫化物出现的金属在硅酸盐熔浆中的溶解度明显增大。

来自于成熟俯冲带的炙热、多水、高氧化度和富含金属元素的玄武质岩浆是含铜岩浆的基本特点。这种含矿岩浆比橄榄质地幔的密度小(Herzberg et al., 1983),所以能够穿透软流圈和上部地幔岩石圈。但是这种上浮力不足以推动含矿岩浆到地表,因而镁铁质岩浆流储存在地壳底部(Glazner and Ussler, 1988). 热传导到周围地壳岩石导致出现地壳熔融(crustal melting),混染作用(assimilation)和均一岩浆的储存(storage of homogenized magma)(即:MASH过程,Hildreth and Moorbath, 1988)。Hildreth和Moorbath(1988)在南美智利中部研究发现地壳对形成斑岩铜矿的贡献,认为这些钙碱性岩浆是楔形地幔部分熔融产生的玄武质岩浆在下地壳下部经历MASH过程(即:熔融、同化、均一、存储)之后所形成。这些概念已经获得广泛接受和应用(例如,杨志明等,2009; Richards, 2003, 2013; Richards and Holm, 2013; Wilkinson, 2013)。该过程的结果形成了杂交化和演化复杂的中性成分岩浆(包括玄武质安山岩和安山岩)。由于其密度低导致可以继续上升,在中上地壳形成大岩体(图8)(Cruden, 1998; Cobbing, 1999; deSaint-Blanquat et al., 2001; Klepeis et al., 2003; Lipman, 2007; Richards and Mumin, 2013),而富含挥发组分的岩浆以岩墙和岩株形式沿脆性断裂侵入浅表,甚至喷发到地表,构成安山岩—英安岩—流纹岩火山弧序列(图9)(Walker, 1989; Jaupart and Allègre, 1991; Carrigan et al., 1992; Eichelberger, 1995; Legros and Kelfoun, 2000; Huppert and Woods, 2002)。

对于岩浆弧斑岩铜矿成矿过程,在前人基础上,Wilkinson(2013)总结提出四个层次的关键作用(图10):其一,在地壳深部具有一个岩浆富集金属和水的过程;其二,岩浆的硫化物饱和过程,致使金属逐步聚集到一个比较小的富矿岩浆系统,随后可以释放出;其三,金属有效地从岩浆转移到出熔的流体系统的过程;最后,金属矿物在地壳的沉淀成矿过程。在这四个关键要素中,岩浆的硫化物是否饱和是形成斑岩型铜矿最关键因素。因此,火成岩的硫化物饱和度可以用于鉴别岩浆是否成矿的关键指标。

成矿物质来源:在岩浆弧环境,钙碱性岩浆通常之所以具有成矿的潜力,大洋板片的脱水无疑是最为关键的过程,该过程不仅把大量的水、硫、卤素、金属,以及亲流体的大离子亲石元素(LILE)输送到地幔楔(Tatsumi et al., 1986; Davidson et al., 1986; de Hoog et al., 2001),同时还因H_2O的大量加入,使得楔形地幔熔融产生的岩浆常具有较高的氧逸度(Richards, 2003)。高氧逸度条件下,则主要以硫酸盐的形式溶解于岩浆之中(盐度约1.5%, Hugo et al., 2001),从而导致通常优先向硫化物分配的Cu, Au等开始作为不相容元素向硅酸盐熔浆中富集(Hamlyn et al., 1985; Bornhost et al., 1986; Richards, 1995,2013),这就是正常钙碱性的弧岩浆常含有较高的亲铜元素(如Cu, Au等)的原因。Campos等(2002)对智利Zaldivar斑岩铜矿床的矿化岩体(即Llamo斑岩体)石英斑晶中的熔融包裹体进行了显微测温和电子探针成分分析,结果表明,这些熔融包裹体富铜但不含硫(低于检测限),其铜含量为0.03%~0.57%,平均为0.1%,比该区正常钙碱性侵入岩高一个数量级,在少数包裹体中还观测到不含硫的铜矿物。因此,Zaldivar斑岩铜矿的铜来自岩浆(Campos et al.,2002)。

PIXE、SXRF、LA ICP-MS等微区分析技术的迅速发展,使斑岩铜矿研究能够以微米级别的精度获取主微量、稀土元素含量以及同位素组成。Wallace和Edmonds(2011)利用LA ICP-MS测定并对比了岩浆硫化物与硅酸盐熔融包裹体的硫含量,精确约束了中酸性岩浆中的硫来源于下部的镁铁质岩浆。Audètat和Simon(2012)进一步测定了镁铁质岩浆岩中熔融包裹体的主微量、稀土元素含量,发现随着岩浆结晶分异的进行,Cu易向岩浆硫化物分配,Mo则向硅酸熔体分配。微区分析技术另外一个重要应用是验证元素在不同相态之间的分馏行为,Zajacz等(2008)报道了多个元素在熔体/气相流体间的分馏系数,Cu元素最高值可达2700,支持了Cu在去气过程中可由气相运移的观点。Pettke等(2010)利用LA ICP-MS微区分析分别获得了美国Bingham矿床铜金矿化、晚期钼矿化阶段

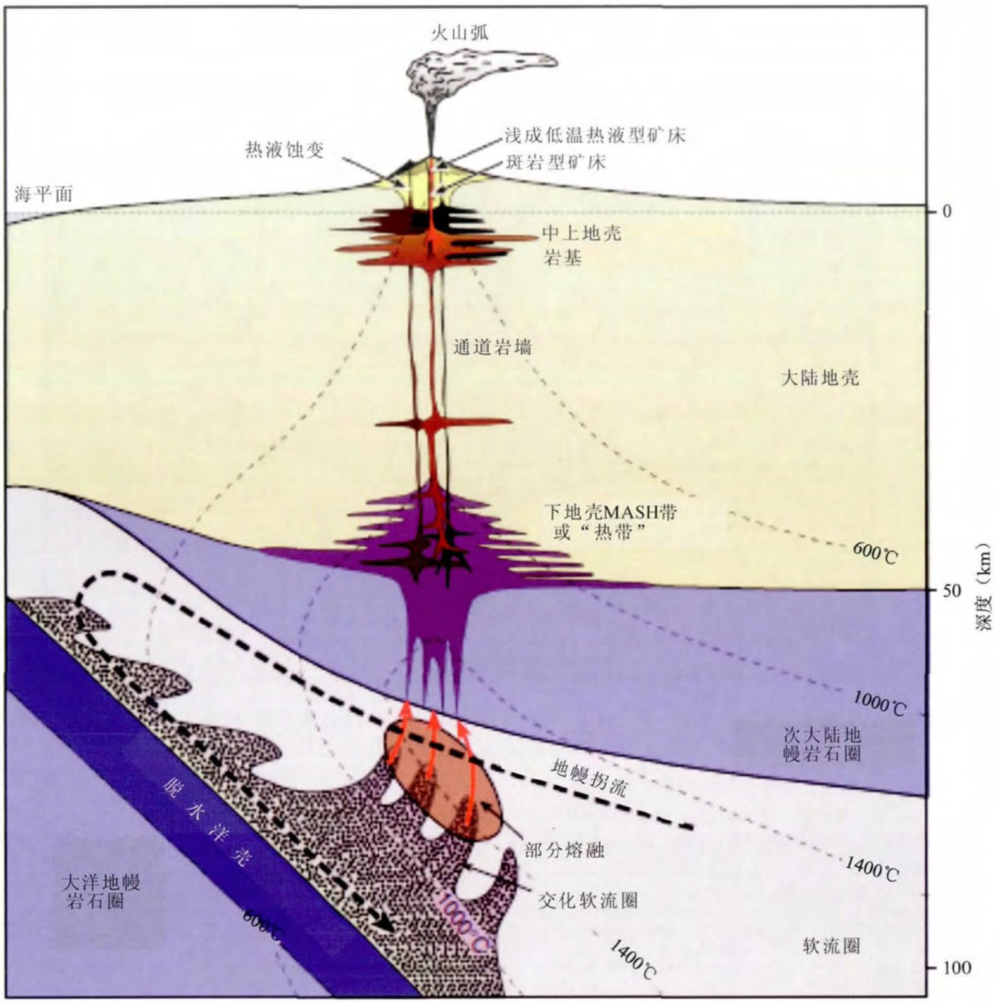

图 8　来自于交代板片的岩浆在下地壳经历了 MASH（熔融、同化、均一、存储）过程，形成高分异和相对低密度岩浆，沿断裂向上运移定位于成矿（据 Richards, 2011）

Fig. 8　Schematic section through a continental arc, showing the development of a MASH or “hot zone” at the base of the crust where basaltic arc magmas pool at their level of neutral buoyancy, differentiate, and interact with crustal rocks and melts. Evolved, less dense, andesitic magmas rise into the mid-to-upper crust where they pool at their new level of neutral buoyancy to form batholithic complexes. Along with volcanic structures, porphyry and epithermal deposits may form at shallower levels above these batholithic complexes where exsolved magmatic fluids ascend, cool, and interact with near-surface upper crustal rock (after Richards, 2011)

中单个流体包裹体的铅同位素组成，证实地幔参与了 Bingham 的铜金钼成矿作用。

3　大陆环境斑岩铜矿

斑岩铜矿除了形成于活动岛弧和大陆边缘外，也出现在大陆内部，空间上可以有两种形式，即：一种是沿古缝合带分布，另一种远离现代或古代缝合带分布，分别可能是碰撞后和板内环境的产物。

Hollister 等（1974）最早注意和研究美国阿巴拉契亚造山带内的斑岩铜矿，发现随着地质历史演化先后形成一组古生代斑岩型矿床，早期为斑岩铜钼矿，晚期为斑岩钼钨矿。与斑岩铜钼矿成矿有关的岩石为石英斑岩、石英二长岩型和石英闪长斑岩，Hollister 等（1974）提出了与石英二长斑岩为核心的矿化蚀变模型，该模型略不同于以美国西南部斑岩铜矿为例建立的经典斑岩铜矿蚀变模型（Lowell and Guilbert, 1970）。在澳大利亚西南威尔士州的 Lachlan 褶皱带发育有 Goonumbla, Endeavour 26 North, Ridgeway 和 Cadia 等斑岩－矽卡岩型铜金矿，Perkins 等（1990）测定 Goonumbla 矿床成矿时代为 439.2 ± 1.2 Ma，Wilson 等（2007）运用锆石 U-Pb 和辉钼矿 Re-Os 方法测定 Ridgeway, Cadia

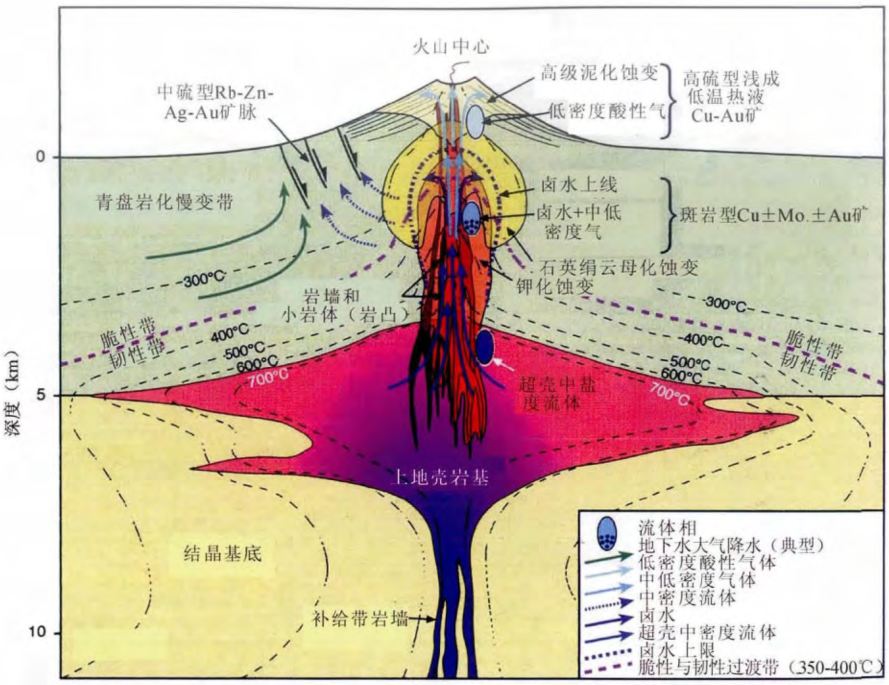

图 9 在中-上地壳岩基、岩隆及火山系统斑岩铜矿 Cu±Mo±Au 矿床-高硫型浅成低温热液型 Cu-Au 矿床及周围中硫型铅锌矿床成矿图解(据 Richards and Mumin，2013)

Fig. 9 Anatomy of a coupled mid- to upper crustal batholith, cupola, volcanic system, showing the level of formation of porphyry Cu ± Mo ± Au deposits, high-sulfidation epithermal Cu-Au deposits, peripheral intermediate-sulfidation Pb-Zn-Ag-Au deposits, and associated hydrothermal alteration(after Richards and Mumin, 2013)

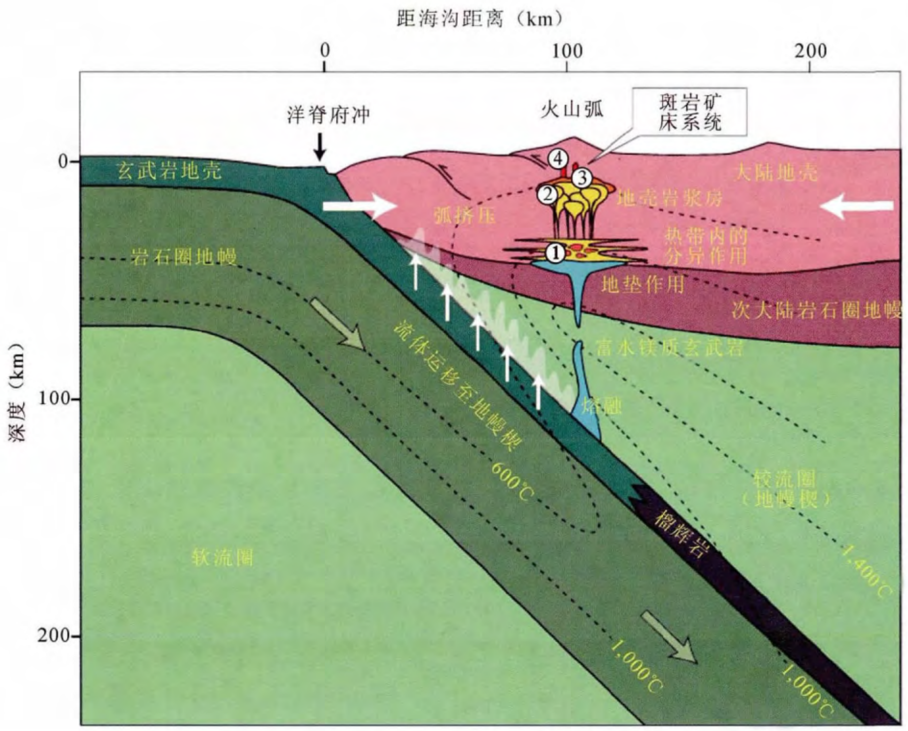

图 10 俯冲带上部斑岩铜矿成矿过程的示意图，导致形成大型斑岩铜矿的四个关键要素(在图中标出的 1～4 在正文解释)(据 Wilkinson，2013)

Fig. 10 Suprasubduction zone setting for the formation of porphyry ore deposits, the four environments where key trigger processes operate that may lead to the formation of large porphyry ore deposits are numbered 1～4 (after Wilkinson, 2013)

Quarry，Cadia Hill 和 Cadia East 几个矿床的时代为 456～454 Ma。Jones (1985)和 Heithersay 和 Walshe (1995)研究认为这组南北向沿火山链分布的斑岩铜金矿位于 Bogan Gate 海槽东部大陆边缘，是于晚奥陶世－早志留世在大陆开裂过程形成。Richards 等 (1990)认为位于大陆－岛弧碰撞带的巴布亚新几内亚 Porgera 碱性斑岩及斑岩金铜矿也是板内环境的产物，形成于大洋板块俯冲的弧后伸展带。Richards(2009，2011，2013)对于斑岩铜矿不同类型成矿环境进行了探索，提出与碰撞岩石圈加厚作用、后碰撞地幔岩石圈拆沉作用和后俯冲岩石圈伸展作用有关形成的斑岩铜矿的成矿物质主要来自俯冲板片交代的地幔岩石圈或早期弧岩浆再造的富水下地壳的残留堆积体。Shafiei 等 (2009)在研究伊朗新生代斑岩铜矿时，也提出成矿物质来自于受交代的次大陆地幔岩石圈。迄今为止，关于在碰撞期间形成的斑岩铜矿较少报道，Cloos 和 Housh (2008)论证新几内亚斑岩铜金矿与碰撞拆沉有着密切的成因联系。伊朗 Kerman 斑岩铜矿带可能是碰撞造山成矿的典例，该斑岩铜矿带形成时代在 29～9Ma，主要峰期在 15～9Ma(Hassanzadeh，1993；McInnes et al.，2003，2005；Taghipour et al.，2008；Aghazadeh et al.，2013；Mirejad et al.，2013)，与碰撞造山时间十分接近。Mohajjel 等 (2003)认为在红海－亚丁湾打开后，阿拉伯半岛与伊朗沿 Zagros 缝合带碰撞对接时间在中新生代。Shafiei 等 (2009)提出新生代中期斑岩及其铜矿是同碰撞期的产物。Mirejad 等 (2013)认为 15Ma 左右的斑岩铜矿形成于碰撞造山期间，而 9Ma 左右的斑岩铜矿形成于碰撞后环境。Haschke 等(2010)进一步研究提出碰撞作用导致弧岩石圈根部拆沉和进而熔融，形成斑岩含矿岩浆和成矿。Sillitoe (2012)总结提出非俯冲有关的三种铜矿成矿的地质构造环境(图 11)，其一，伴随拆沉岩石圈地幔下沉到软流圈过程，受交代岩石圈地幔和俯冲停止后软流圈上涌期间的下地壳部分熔融形成斑岩铜矿岩浆；其二，大陆碰撞后含铜岩浆弧风化剥蚀后，在陆内伸展盆地内沉积形成砂岩铜矿；其三，在地幔柱活动期间来自富铜岩石圈地幔或下地壳的 IOCG 矿产有关岩浆在板内成矿。

位于欧亚大陆东南部的我国，尽管已发现的斑岩铜矿规模虽然不大，但数量众多，在地质历史期间呈多幕次分布(芮宗瑶等，1984；Mao et al.，2014)。因此，我国学者对于大陆斑岩铜矿研究起始较早，正如张洪涛等(2013)所总结："芮宗瑶等(1984)提出斑岩铜矿的形成是壳幔长期作用的产物，在大陆板块边缘弧(陆缘弧)环境和大洋板块边缘弧(岛弧)环境都能形成斑岩铜矿，汇聚板块边缘的造山作用提供了最有利的成矿背景"，特别指出"陆-陆碰撞造山作用同样具有成矿前提"。芮宗瑶和张洪涛(1986)把分布于我国东部大陆边缘和西南部的印支、燕山和喜马拉雅期褶皱带中的斑岩铜矿称为造山期后斑岩铜矿床，并概要提出其矿化蚀变模式。真允庆(1999)、芮宗瑶等(1984)、黄崇轲等(2001)认为并非所有的斑岩铜矿床都产于造山过程，有些可能与大陆裂谷作用有关，如中国中条山铜矿床。张洪涛等(2004)认为，"中国东部中生代斑岩铜矿的成因，虽与太平洋板块向西的俯冲作用有关，但更直接的成矿地质作用则是岩石圈地幔的活化减薄；西藏冈底斯成矿带则是碰撞后的产物"。

过去 10 多年，埃达克岩与斑岩铜矿成矿在我国产生了重大影响，推动了我国对大陆斑岩铜矿的深入探索。张旗等(2001，2004)研究提出大陆埃达克岩(或 C 型埃达克岩)新概念，认为其成因 C 型埃达克岩富 K(大部分仍然是钠质的，少数为钾质的)，可能是玄武岩底侵到加厚的陆壳(＞50km)底部导致的下地壳麻粒岩部分熔融的产物。与来自俯冲洋壳板片重熔的埃达克岩类同，运用高 Sr 低 Y(或 Yb)特点可以有效辨别出 C 型埃达克岩，并论证为"埃达克岩有利于成矿的关键因素与埃达克岩形成时角闪石转变为石榴石的脱水作用有关，而水能萃取出在地幔和基性岩中富集的金属元素"。Hou 等(2004)将冈底斯斑岩铜矿带中与成矿有关的钙碱性-高钾钙碱性花岗质岩石论证为埃达克岩，并提出新生加厚的镁铁质下地壳是大陆斑岩铜矿的成矿物质源区(Hou et al.，2009，2011，2013)。侯增谦等(2007，2009)划分出后碰撞、后造山和非造山三种类型大陆斑岩铜矿，并提出模型图(图 12)，其核心是成岩成矿物质与俯冲板片无关，而是来自新生下地壳或由于软流圈上侵导致壳幔相互作用所产生的熔浆。最近，Zhou 等(2014)通过对长江中下游地区斑岩－矽卡岩型铜多金属矿带的研究，提出它们是一种典型的陆内斑岩铜矿，其成矿岩浆是来自富集地幔的基型岩浆与加厚下地壳部分熔融的长英质岩浆混合岩浆，而富集地幔岩浆提供了成矿所必须的 H_2O，S 和金属元素 Cu 和 Au 等。

目前关注的焦点问题：与俯冲环境成矿不同，对于大陆斑岩铜矿的成矿作用在某些方面仍然存在一

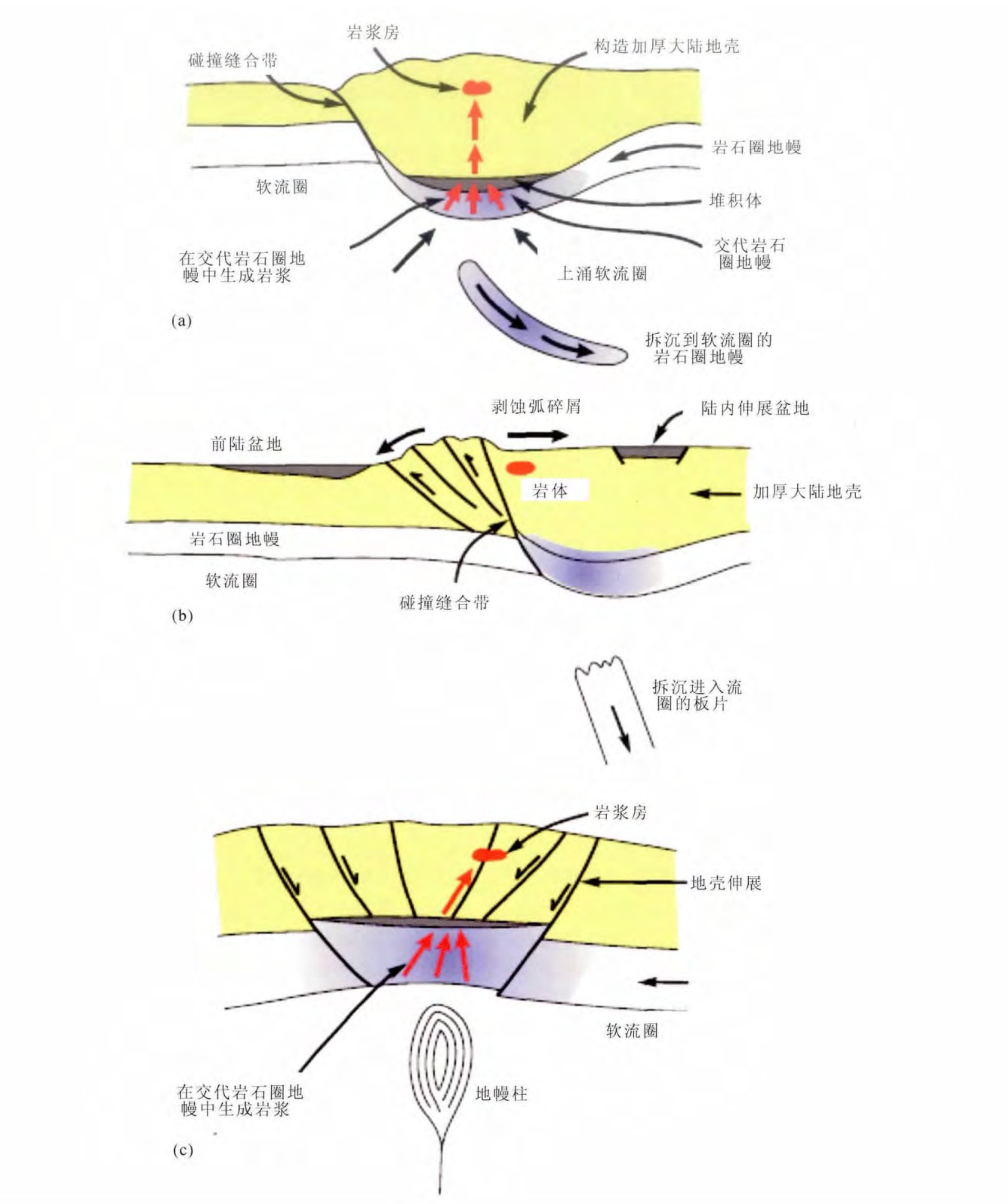

图 11 非俯冲环境形成铜矿的地质构造环境(a,b,c **解释见正文**)(**据** Sillitoe, 2012)

Fig. 11 Cartoons of additional geotectonic scenarios that could be influential in major copper deposit/province formation(after Sillitoe, 2012)

些不同的认识,主要表现在以下两个方面:

板内成矿——低角度及平板俯冲成矿还是陆内俯冲成矿:在 20 世纪 70～80 年代,对于大陆内部的矿产统称为板内成矿作用的产物,其形成机制曾困扰着人们。例如,像美国西南部的斑岩铜矿集中区,其分布范围从俯冲海沟向东经加利福尼亚州、亚利

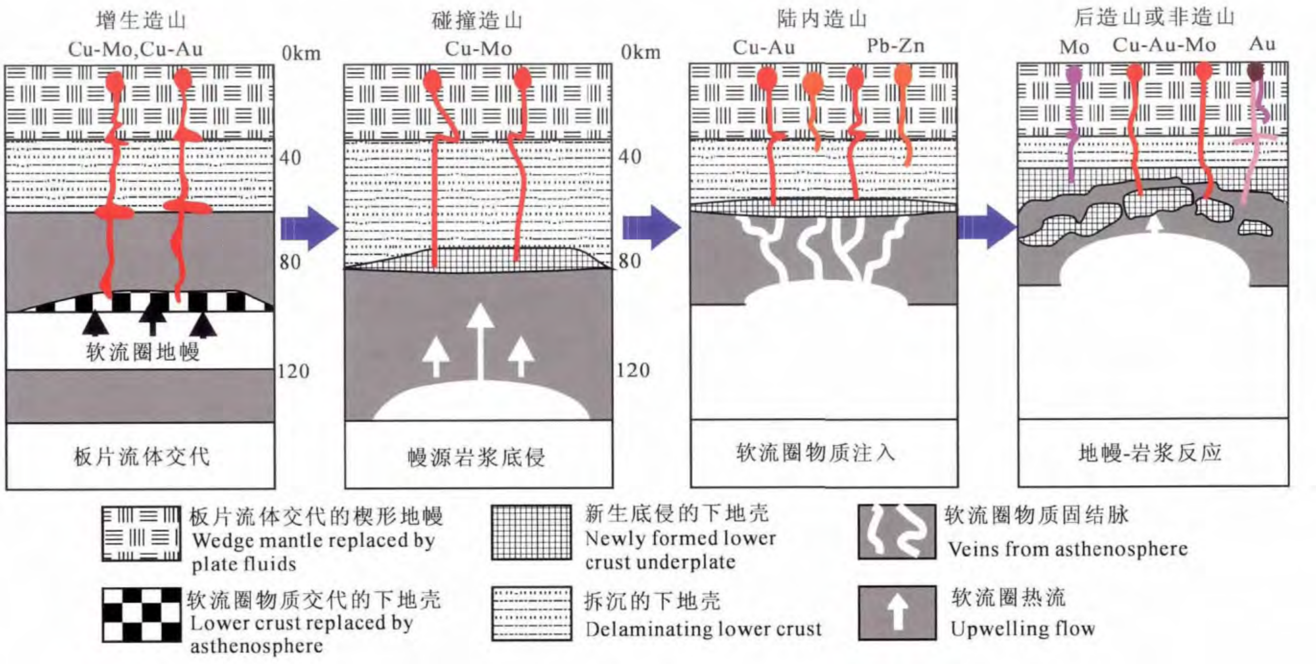

图 12　大陆斑岩铜矿成矿构造环境示意图(据侯增谦等,2009)

Fig. 12　Simplified profiles illustrating the lithospheric structures in different evolved stages of continental tectonics and showing possible sources for metals and magmas associated with porphyry-type deposits in non-arc settings (after Hou et al., 2009)

桑那州到德克萨斯州,向北达到犹他州的 Bingham Canyon,直径均长达 1500km,斑岩铜矿多出现在盆岭构造的伸展盆地内。与部分斑岩铜矿同时代的矿产还有内华达州盆岭构造盆地中的卡林型金矿和科罗拉多州弧后盆地的斑岩钼矿。因此,当时大多数学者(例如,Livingston et al., 1973; Lowell et al., 1974)强烈质疑俯冲板块形成斑岩铜矿的构造模型(Sillitoe, 1972),认为在板内伸展环境上地幔或下地壳来源的岩浆沿地壳薄弱地带上升定位与成矿,可以更好地解释北美西南地区斑岩铜矿和斑岩钼矿的成矿作用和分布规律。进而,Davies(1989)发现整个北美西部矿产围绕北美克拉通从东向西成矿时代逐渐变年轻,分别为 200Ma,150Ma 和 80～40Ma,认为成矿与地块增生有密切关系。尽管对于沿着克拉通构造如何增生的机制尚不清楚,但很明显沿着克拉通深部的构造控制着 NW 向壳幔反应带及其发生地幔上涌,就是在克拉通与增生体之间这几条薄弱地带成为斑岩铜矿成矿的空间。进入 20 世纪 80 年代后,越来越多证据表明斑岩铜矿与俯冲板块的成因联系,例如,Titley 和 Beane (1981),Titley (1993)认为在晚白垩世期间,当板块快速俯冲停止和斜向俯冲变成主要方式后,北美板块相对于太平洋板块发生右旋,因此出现大量控制斑岩铜矿的伸展构造体系。直到 2000 年左右,随着岩石地球化学、深部地球物理和地球动力学模拟研究的深入开展,板块低角度及平板俯冲及与成矿作用越来越被接受(Gutscher et al., 2000),而且与之有关形成诸多大型—超大型斑岩铜矿、斑岩钼矿以及钨锡多金属矿产(Sillitoe, 1998, 2013; Kerrich et al., 2000; Kirkham and Dunne, 2000;Cooke et al., 2005)。

我国东部大陆内部一系列斑岩铜矿也是远离大洋,尽管目前不能完全确定中晚侏罗世—早白垩世的俯冲海沟当时在什么位置。即使在大陆边缘,斑岩铜矿出现在内陆延伸近 1000 km。由此以来,我国长期将这些斑岩铜矿称为大陆斑岩铜矿,由大陆内部壳幔相互作用而形成。戚建中(1990)、戚建中等(2000)注意到太平洋板块俯冲和走滑与我国东部燕山期成矿作用的成因关系。过去 10 多年,我国学者从构造地质、岩石学和矿产地质等方面的研究(万天丰和朱鸿,2002;万天丰,2004;万天丰等,2008;毛景文等,2003, 2004a,2004b, 2005, 2008;Mao et al., 2002, 2006, 2008, 2011a, 2011b, 2011c, 2011d, 2013, 2014;赵越等,2004;董树文等,2007,张岳桥等,2009)厘定东部大陆构造体制经历了两次大转变,即在 170Ma 左右从特提斯南北向挤压体制

转换为太平洋斜向俯冲体制，形成大规模斑岩－矽卡岩铜矿、钼矿和钨锡多金属矿产，在 135Ma 左右大陆表现以走滑－伸展为主，135～80Ma 形成的大多数斑岩铜矿－浅成低温热液型金银矿及锡矿和铅锌矿，主要出现在一系列伸展盆地或走滑拉分盆地中。在挤压体制中的斑岩铜矿主要来自撕裂的俯冲板片，而在伸展体制中斑岩铜矿主要来自后俯冲残留板片或受交代的次大陆岩石圈地幔。最近几年，Ling 等（2009），Sun 等（2010，2014）研究提出长江中下游斑岩和华南地区的中生代斑岩铜矿与洋中脊俯冲关系密切，洋中脊俯冲提供了能量和物质来源。

碰撞后成矿——成矿物质来自于陆内壳幔相互作用的产物（或新生铁镁质下地壳）还是残留俯冲板片引致的交代地幔：尽管对大陆斑岩铜矿研究有 40 多年历史，但是，其成矿成岩物质来源在近 10 年成为关注的焦点。在我国，长期以来大家普遍认为大陆斑岩铜矿的物质主要来自陆内的壳幔相互作用，成矿物质源于下地壳和上地幔。最近几年，不少学者论述大陆斑岩铜矿主要来自新生下地壳，并开展了大量积极的探索（例如，Hou et al.，2009，2011，2013；Xu et al.，2014；Yang et al.，2014）。

如前所述，在国外，无论是碰撞、后碰撞还是后俯冲环境，斑岩铜矿的成矿物质来源被认为与前期大洋板块俯冲关系密切，残留的大洋板片重熔并交代次大陆岩石圈，甚至下地壳形成含矿岩浆（例如，Shafiei et al.，2009；Richards，2009，2011，2013；Sillitoe，2012）。在我国也存在类似的认识，认为俯冲板片为大陆斑岩铜矿成矿不仅提供了大量铜元素来源，而且也提供了丰富的流体（例如，Qu et al.，2004，2007；Mao et al.，2011a，2013，2014；Zheng et al.，2014；Wang et al.，2014）。这些残留板片不仅是碰撞前俯冲板片的残余，也可能是早期不同构造体制下残留的古老洋壳板片。例如，Liu 等（2012）研究提出德兴斑岩铜矿的成矿物质可能来自于新元古代扬子与华夏碰撞对接前华南大洋板片的残留体。又如，哀牢山－红河新生代的斑岩铜金矿成矿物质可能主要来自于三叠纪残留的大洋板片交代岩石圈（Lu et al.，2013；Tran et al.，2014；Liu et al.，2014）。

事实上，运用岩石地球化学很难鉴别与斑岩铜矿有关花岗质岩石的物质来源，由于新生下地壳、交代岩石圈地幔、甚至大洋板片的物质成分，具有类似的岩石化学、Sr-Nd-Hf 同位素特征。之所以强调交代岩石圈对成矿的贡献主要考虑三种因素：其一，几乎所有的碰撞、后碰撞和后俯冲有关的斑岩铜矿大多数出现在造山带，沿古老结合带两侧分布，少数出现在活动大陆边缘（例如，我国东部 135～80Ma 的斑岩铜矿－浅成低温热液型金银矿系统）；其二，洋壳更加富含铜元素，可达 86×10^{-6}，而原始地幔 30×10^{-6}，亏损地幔 29.1×10^{-6} 和下地壳 26×10^{-6}（韩吟文等，2003）；其三，也是更重要的一点是大洋板片俯冲过程把大量海底沉积物，水和硫化物携带到软流圈，以至于发生交代作用，形成含矿岩浆。俯冲有关的岩浆通常至少含有 4% H_2O（Burnham，1979；Naney，1983；Rutherford and Devine，1988），Oyarzun 等（2001）认为相对于来自软流圈部分重熔的岩浆，俯冲板片熔融的岩浆异乎寻常地被氧化且富集 H_2O 和 SO_2，这种岩浆特别易于在上地壳形成岩浆－热液的斑岩铜矿系统。

4 矿床模型与找矿勘查

矿床模型是找矿勘查过程总结出的理论卡通模型，可以有效地指导进一步找矿勘查。在斑岩铜矿勘查与研究早期，Lowell 和 Gilbert（1970）根据蚀变特征及其分带，提出了注明斑岩铜矿蚀变分带模型（图 13）。该模型不仅对于开展找矿勘查具有重要指导意义，并取得了很好的效果，而且可以有助于判别斑岩铜矿系统的剥蚀风化程度. 例如，如果在矿区有大量钾长石化发育，就表明该斑岩铜矿已经风化到下部或者接近残留根部，进一步找矿效果将很有限。在 20 世纪 90 年代，通过对西南太平洋斑岩铜金矿和浅成低温热液型金银矿的研究，发现两者之间有着密切的联系，Hedenquist 和 Lowenstern（1994）提出了斑岩铜矿－浅成低温热液型金矿床模型（图 14），包括下部的斑岩铜金矿，上部高硫型浅成低温热液型金矿和外围的低硫型浅成低温热液型金银矿。该模型对于全球开展铜金矿找矿勘查起到了重要的指导作用，从此浅成低温热液型金矿成为主要金矿类型之一，也成为找矿的重要目标。在我国，紫金山矿田就是一个很好地范例，首先探明了紫金山高硫型浅成低温热液型铜金矿，接着在其外围发现和探明悦洋（碧田）低硫型浅成低温热液型银金矿，最近几年又探明了罗卜岭斑岩铜钼矿（张锦章，2013）。最近几年，在班公湖－怒江成矿带探明了荣纳大型斑岩－高硫型浅成低温热液型铜金矿，目前正进一步勘查之中。

斑岩铜矿在形成过程中，如果围岩是碳酸盐岩，

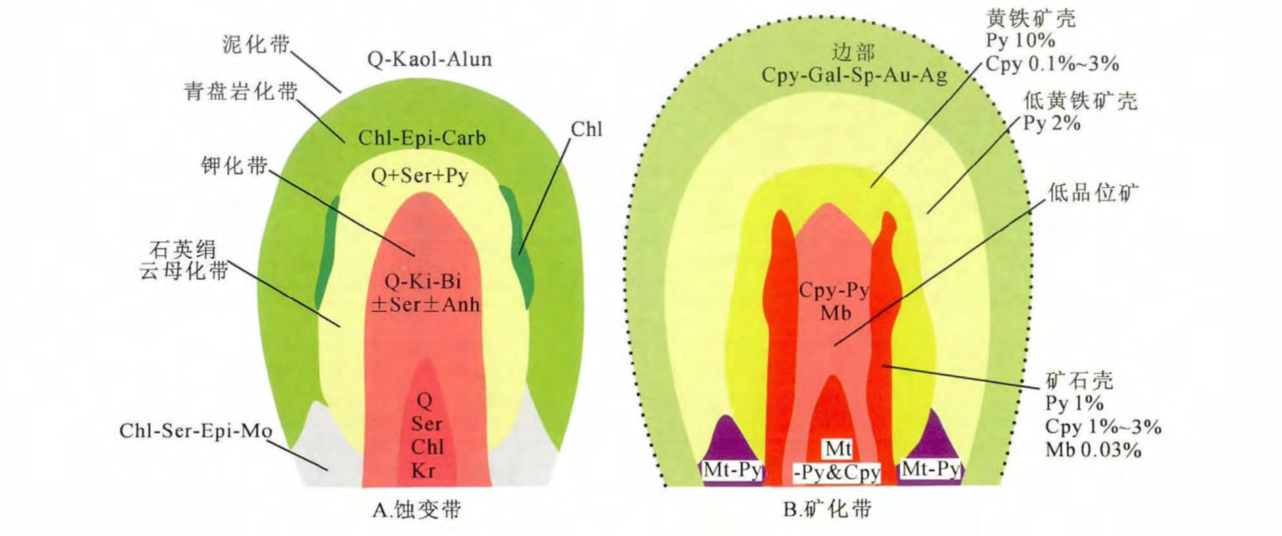

图 13 斑岩铜矿矿化蚀变分带图(据 Lowell and Guilbert, 1970; Sun et al., 2014)

Fig. 13 Mineralization-alteration zonings of porphyry Cu deposit (after Lowell and Guilbert, 1970; Sun et al., 2014)

Chl—绿泥石;Kaoli—高岭石;Epi—绿帘石;Alun—明矾石;Carb—碳酸盐岩化;Bi—黑云母;Q—石英;Ser—绢云母;Kf—钾长石;Py—黄铁矿;Cpy—黄铜矿;Gal—方铅矿;Sp—闪锌矿;Au—金;Ag—银;Mb—辉钼矿;Anh—硬石膏

Chl—chlorite;Kaoli—kaolinite;Epi—epidote;Alun—alunite;Carb—carbonate;Bi—biotite;Q—quartz;Ser—sericite;Kf—feldspar;Py—pyrite;Cpy—chalcopyrite;Gal—galena;Sp—sphalerite;Au—gold;Ag—silver;Mb—molybdenite;Anh—anhydrite

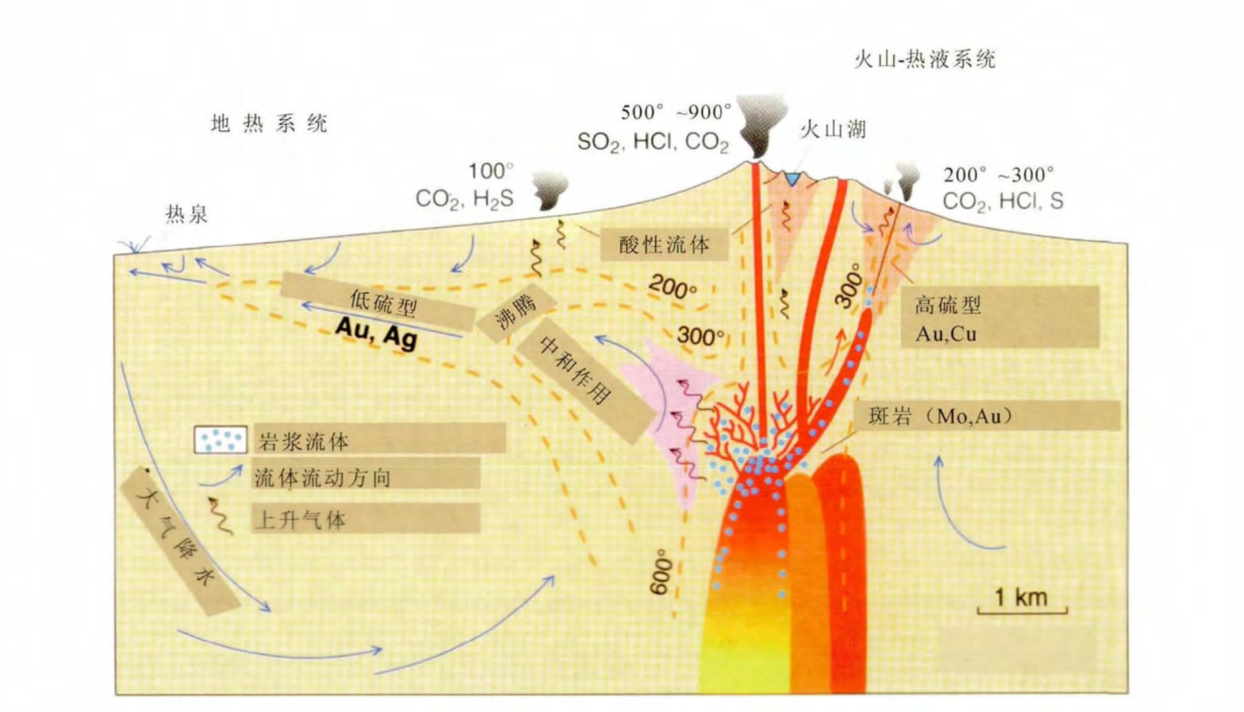

图 14 斑岩铜矿-浅成低温热型金矿成矿模型图(据 Hedenquist and Lowenstern, 1994)

Fig. 14 Model ofporphyry Cu-epithermal Au deposits (after Hedenquist and Lowenstern, 1994)

成矿流体与围岩相互作用,形成矽卡岩型铜矿,沿层交代出现 Manto 型铜铅锌矿,甚至脉状铅锌银矿以及低温热液脉型金银锑汞矿。据此,Silittoe (2010) 研究提出了一个新的模型(图 15),表明以斑岩铜矿为核心,向上有浅成低温热液型金银矿,向上或向外,在沉积岩中发育有铅锌银锑汞矿,因此,有力地推动了综合找矿勘查的开展。显而易见,与单个矿床模型相比,矿集区矿床模型具有更多优点,对于找

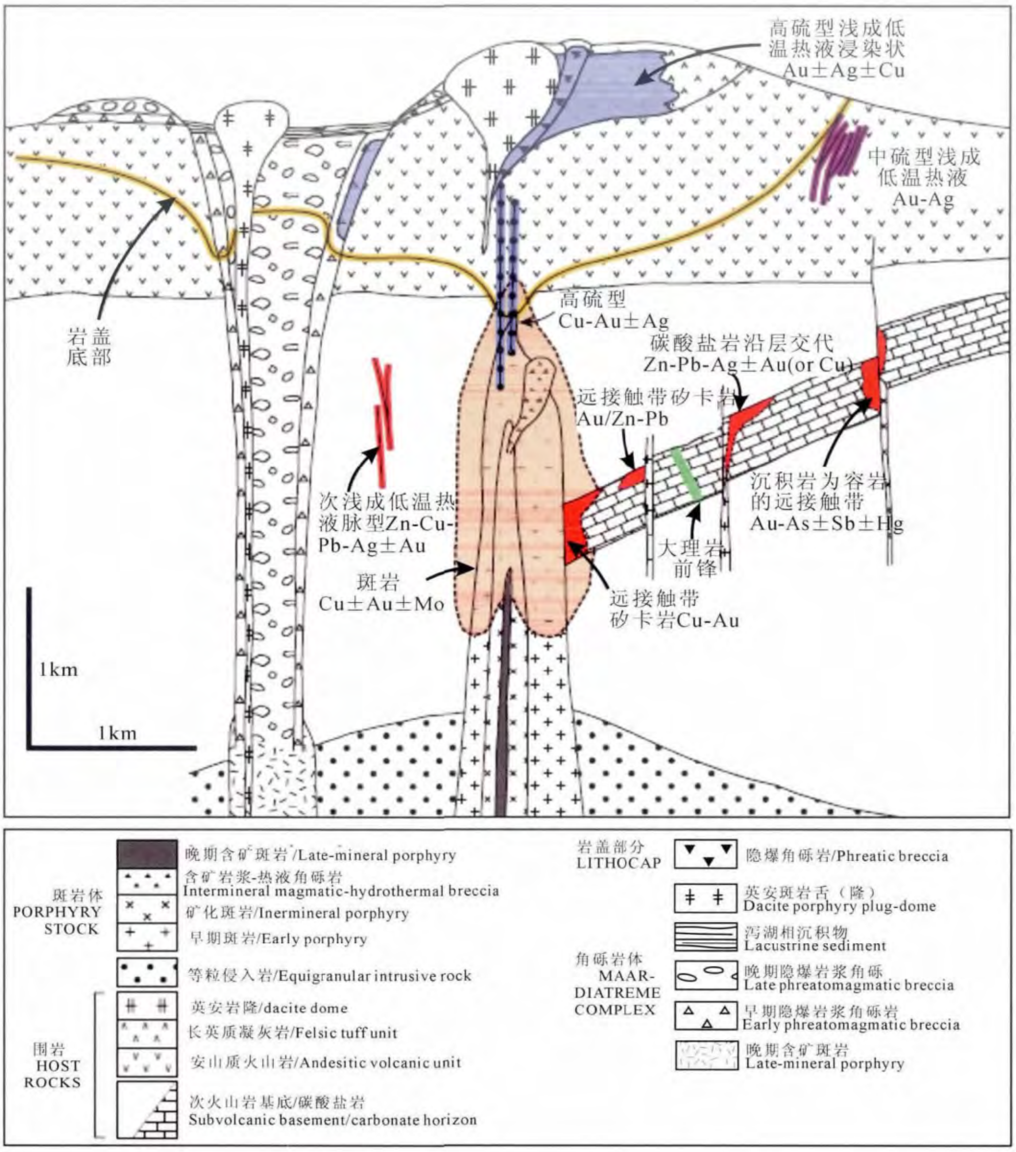

图 15 斑岩-矽卡岩-浅成低温热液型多金属矿床成矿模型图(据 Sillitoe, 2010)

Fig. 15 Anatomy of a telescoped porphyry Cu system showing spatial interrelationships of a centrally located porphyry Cu± Au ± Mo deposit in a multiphase porphyry stock and its immediate host rocks; peripheral proximal and distal skarn, carbonate-replacement (chimney-manto), and sediment-hosted (distal-disseminated) deposits in a carbonate unit and subepithermalveins in noncarbonate rocks; and overlying high- and intermediate-sulfidation epithermal deposits in and alongside the lithocap environment(after Sillitoe, 2010)

矿勘查具有更重要的指导意义。毛景文等(2009, 2010)根据在铜陵矿集区和德兴矿集区的研究结果，提出了斑岩－矽卡岩－沿层交代型铜多金属矿床模型和斑岩铜矿－浅成低温热液型银铅锌－远接触带金矿床模型。杨志明和侯增谦(2009)以冈底斯后碰撞斑岩铜矿带研究为基础，提出了一个综合性矿床模型。这些模型对于目前我国在斑岩铜矿带和在开采的矿山进一步找矿勘查都具有重要的引导性。

最近几年，澳大利亚塔斯马尼亚大学 David Cooke 教授领导的科研团队致力于与矿业公司合作，针对斑岩铜矿系统中的蚀变矿物，开展 Footprint(找矿印痕)研究，取得了初步成果。主要原理是利用常见的蚀变矿物，例如，绿泥石、绿帘石、明矾石和粘土矿物等进行成分和形成物理化学条件的测定，探讨这些与成矿有关矿物的特征及其空间的分布规律，提出进一步找矿的标志。Chang 等(2011)在这方面开展了先导性研究，取得了好的效果。

后记：今年是我国著名矿床地质学家，笔者尊敬的老师，陈毓川院士 80 华诞，特此撰写此文，表示热烈恭贺。由于笔者从事斑岩铜矿研究时间不够长，对全球该方面研究和勘查历史和现状了解的尚不够全面，对于不少新认识理解不够深入，尽管力图客观提供有关信息，也难免有不当之处，敬请批评指正。

参 考 文 献

陈华勇，肖兵. 2014. 俯冲边界成矿研究进展及若干问题. 地学前缘，21(5)：13～22.
董树文，张岳桥，龙长兴，杨振宇，季强，王涛，胡建民，陈宣华. 2007. 中国侏罗纪构造变革与燕山运动新诠释. 地质学报，81(11)：1449～1461.
韩吟文，马振东，张鸿飞，等. 2003. 地球化学. 北京：地质出版社，33～47.
黄崇轲，白冶，朱裕生. 2001. 中国铜矿床. 北京：地质出版社，57～198.
侯增谦，潘小菲，杨志明，曲晓明. 2007. 初论大陆环境斑岩铜矿. 现代地质，21：332～351.
侯增谦，杨志明. 2009. 中国大陆环境斑岩型矿床：基本地质特征、岩浆热液系统和成矿概念模型. 地质学报，83：1779～1816.
毛景文，张作衡，余金杰，王义天，牛宝贵. 2003. 华北及邻区中生代大规模成矿的地球动力学背景：从金属矿床年龄精测得到启示. 中国科学(D 辑)，33 (4)：289～300.
毛景文，Stein H，杜安道，周涛发，梅燕雄，李永峰，藏文栓，李进文. 2004a. 长江中下游地区铜金(钼)矿 Re-Os 年龄测定及其对成矿作用的指示. 地质学报，78(1)：121～131
毛景文，谢桂青，李晓峰，张长青，梅燕雄. 2004b. 华南地区中生代大规模成矿作用与岩石圈多阶段伸展. 地学前缘，11 (1)：45～55.
毛景文，谢桂青，张作衡，李晓峰，王义天，张长青，李永峰. 2005. 中国北方中生代大规模成矿作用的期次及其地球动力学背景. 岩石学报，21：169～188.
毛景文，谢桂青，郭春丽，袁顺达，程彦博，陈毓川. 2008. 华南地区中生代主要金属矿床时空分布规律和成矿环境. 高校地质学报，14：510～526.
毛景文，邵拥军，谢桂青，张建东，陈毓川. 2009. 长江中下游成矿带铜陵矿集区铜多金属矿床模型. 矿床地质，28(2)：109～119。
毛景文，张建东，郭春丽. 2010. 斑岩铜矿-浅成低温热液银铅锌-远接触带热液金矿矿床模型：一个新的矿床模型—以德兴地区为例. 地球科学与环境学报，32：1～14.
毛景文，陈懋弘，袁顺达，郭春丽. 2011. 华南地区钦杭成矿带地质特征和矿床时空分布规律. 地质学报，85(5)：636～658
毛景文，张作衡，王义天，等，2012. 国外主要矿床类型、特点及找矿勘查. 北京：地质出版社，189～244.
戚建中. 1990. 中国东南燕山期内生金属成矿地动力背景探讨. 中国地质科学院南京地质矿产研究所所刊，11(4)：1～15.
戚建中，刘红樱，姜耀辉. 2000. 中国东部燕山期俯冲走滑体制及其对成矿定位的控制. 火山岩地质与成矿，21(4)：244～265.
芮宗瑶，侯增谦，曲晓明，张立生，王龙生，刘玉琳. 2003. 冈底斯斑岩铜矿成矿时代及青藏高原隆升. 矿床地质，22：217～225.
芮宗瑶，黄崇轲，齐国明，徐珏，张洪涛. 1984. 中国斑岩铜钼矿床. 北京：地质出版社，279～292.
芮宗瑶，张洪涛. 1986. 试论中国斑岩型矿床系列. 中国地质科学院院报，14：89～99.
唐菊兴，邓世林，郑文宝，应立娟，汪雄武，钟康惠，秦志鹏，丁枫，黎枫佶，唐晓倩，钟裕峰，彭慧娟. 2011. 西藏墨竹工卡县甲玛铜多金属矿床勘查模型. 矿床地质，30(2)：179～196.
涂光炽等，1989. 关于富碱侵入岩. 矿产与地质，3(3)：1～4.
万天丰，朱鸿. 2002. 中国大陆及邻区中生代—新生代大地构造与环境变迁. 现代地质，16(2)：107～120.
万天丰. 2004. 侏罗纪地壳转动与中国东部岩石圈转型. 地质通报，23(9)：966～972.
万天丰，王亚妹，刘俊来. 2008. 中国东部燕山期和四川期岩石圈构造滑脱与岩浆起源深度. 地学前缘，15(3)：1～35.
王植，闻广. 1957. 中条山式斑岩铜矿. 地质学报，37(4)：401～415.
杨志明，侯增谦，宋玉财，李振清，夏代详，潘凤雏. 2008. 西藏驱龙超大型斑岩铜矿床：地质、蚀变与成矿. 矿床地质，27：279～318.
杨志明，侯增谦. 2009. 初论碰撞造山环境斑岩铜矿成矿模型. 矿床地质，28：515～538.
姚春亮，陆建军，郭维民，袁林，李伟. 2007. 斑岩铜矿若干问题的最新研究进展. 矿床地质，26：221～229.
张锦章. 2013. 紫金山矿集区地质特征、矿床模型与勘查实践. 矿床地质，32：757～766.
张洪涛，陈仁义，韩芳林. 2004. 重新认识中国斑岩铜矿的成矿地质条件. 矿床地质，23：150～163.
张洪涛，陈仁义，舒思齐. 2013. 中国大陆斑岩铜矿若干问题. 矿床地质，38：672～684.
张旗，王焰，钱青，杨进辉，王元龙，赵太平，郭光军. 2001. 中国东部中生代埃达克岩的特征及其构造一成矿意义. 岩石学报，17：236～244.
张旗，秦克章，王元龙，张福勤，刘红涛，王焰. 2004. 加强埃达克岩研究，开创中国 Cu、Au 等找矿工作的新局面. 岩石学报，20(2)：195～204.
张岳桥，徐先兵，贾东，舒良树. 2009. 华南早中生代从印支期碰撞构造体系向燕山期俯冲构造体系转换的形变记录. 地学前缘，16：234～247.
赵越，徐刚，张拴宏，杨振宇，张岳桥，胡健民. 2004. 燕山运动与东亚构造体制的转变. 地学前缘，11(3)：319～328.
真允庆. 1999. 中条裂谷铜矿床的成矿规律及其找矿方向. 桂林工学院学报，19：9～18.
郑有业，薛迎喜，程力军，樊子珲，高顺宝. 2004. 西藏驱龙超大型斑岩铜(钼)矿床：发现、特征及意义. 地球科学，29：103～108.
Aghazadeh M，Hou Z，Badrzadeh Z. 2013. Bondar-e-Honza：An oldest and special porphyry copper (molybdenum) deposit in the Kerman porphyry copper belt，Iran. GSA conference，Sweden.
Audétat A，Simon A. 2012. Magmatic controls on porphyry copper deposits. Society of Economic Geologists，Inc. Special Publication，16，573～618.
Ballhaus C. 1993. Redox states of lithospheric and asthenospheric upper mantle. Contributions to Mineralogy and Petrology，114：331～348.
Barra F，Valencia V A. 2014. Late Cretaceous porphyry copper mineralization in Sonora，Mexico：Implications for the evolution of the Southwest North America porphyry copper province. Mineralium Deposita，49：879～884.
Bornhorst T J，Rose W I. 1986. Partitioning of gold in calc-alkaline volcanic rocks from Gutemala. Journal of Geology，94：412～418.
Botcharnikov R E，Linnen R L，Wilke M，Holtz F，Jugo P J，

Berndt J. 2011. High gold concentrations in sulphide-bearing magma under oxidizing conditions. Nature Geoscience, 4: 112～115.

Brandon A D, Draper D S. 1996. Constraints on the origin of the oxidation state of mantle overlying subduction zones: An example from Simcoe, Washington, USA. Geochimica et Cosmochimica Acta, 60: 1739～1749.

Burnham C W. 1967. Hydrothermal fluids at the magmatic stage, in Barnes, H. L., ed., Geochemistry of hydrothermal ore deposits: New York, Holt, Rinehart and Winston, 34～76.

Burnham C W. 1979. Magmas and hydrothermal fluids, In: Barnes, H. L. (Ed.) Geochemistry of Hydrothermal Ore Deposits, 2nd edition. John Wiley and Sons, New York, 71～136.

Campos E, Touret J L R, Nikogosian I, Dalgado J. 2002. Overheated, Cu-bearing magma in the Zaldivar porphyry Cu deposit in North Chile: Geodynamic consequences. Tectonophysics, 345(1～4): 229～251.

Carrigan C R, Schubert G, Eichelberger J C. 1992. Thermal and dynamical regimes of single-and two-phase magmatic flow in dikes. Journal of Geophysical Research, 97: 17377～17392.

Cervantes P, Wallace P J. 2003. Role of H_2O in subduction-zone magmatism: New insights from melt inclusions in high-Mg basalts from central Mexico. Geology, 31: 235～238.

Chen X H, Seitmuratova E, Wang Z H, Chen Z L, Han S Q, Li Y, Yang Y, Ye B Y, Shi W. 2014. SHRIMP U-Pb and Ar-Ar geochronology of major porphyry and skarn Cu deposits in the Balkhash Metallogenic Belt, Central Asia, and geological implications. Journal of Asian Earth Sciences, 79 (Part B):723～740.

Chang Z S, Hendenquist J, White N C, Cooke D R, Roach M, Deyell C L, Garcia J R, Gemmell J B, McKnight S, Cuison L. 2011. Exploration tools for linked porphyry and epithermal deposits: Example from the Mankayan intrusion-centered Cu-Au district, Luzon, Philippines. Economic Geology, 106: 1365～1398

Chiu H Y, Chung S L, Zarrinkoub M H, Mohammadi S S, Khatib M M., Iizuka Y. 2013. Zircon U-Pb age constraints from Iran on the magmatic evolution related to Neotethyan subduction and Zagros orogeny. Lithos, 162～163: 70～87.

Ciobanu C L, Nigel J, Cook N J, Stein H. 2002. Regional setting and geochronology of the Late Cretaceous Banatitic Magmatic and Metallogenetic Belt. Mineralium Deposita, 37: 541～567.

Cloos M, Housh T B. 2008. Collisional delamination: Implications for porphyry-type Cu-Au ore formation in New Guinea. Arizona Geological Society Digest, 22: 235～244.

Cobbing E J. 1999. The Coastal Batholith and other aspects of Andean magmatism in Peru. Geological Society of London, Special Publication, 168:111～122.

Cooke D R, Hollings P, Walsh J L. 2005. Giant porphyry deposits: characteristics, distribution, and tectonic controls. Economic Geology, 100 (5): 801～818.

Cooke D, Hollings P, Holliday J. 2008. Circum-Pacific Porphyry Copper, Gold and Molybdenum Deposits//Committee of 2008. Pacific Rim Congress. The Pacific Rim: Mineral Endowment, Discovery and Exploration Frontiers. Carlton South Australasian Institute of Mining and Metallurgy, 7～14.

Cruden A R. 1998. On the emplacement of tabular granites. Geological Society of London Journal, 155: 853～862.

Davidson J P. 1996. Deciphering mantle and crustal signature of subduction zone magmatism. Geophysical Monograph, 96: 251～262.

Davies J F. 1989. Some temporal-spatial aspects of North American porphyry deposits. Economic Geology, 84: 2300～2306.

Davies J F, Luhta L E. 1978. An Archean "porphyry-type" disseminated copper deposit, Timmins, Ontario. Economic Geology, 73: 383～396.

de Hoog J C M, Hattori K H, Hoblitt R P. 2004. Oxidized sulfur-rich mafic magma at Mount Pinatubo, Philippines: Contributions to Mineralogy and Petrology, 146: 750～761.

de Hoog J C M, Mason P R D, van Bergen M J. 2001. Sulfur and chalcophile elements in subduction zones: Constraints from a laser ablation ICP-MS study of melt inclusions from Galunggung Volcano, Indonesia. Geochimica et Cosmochimica Acta, 65: 3147～3164.

de Saint-Blanquat M, Law R D, Bouchez J L, Morgan S S. 2001. Internal structure and emplacement of the Papoose Flat pluton: An integrated structural, petrographic, and magnetic susceptibility study: Geological Society of America Bulletin, 113: 976～995.

DeBari S M, Sleep N H. 1991. High-Mg, low-Al bulk composition of the Talkeetna island arc, Alaska: Implications for primary magmas and the nature of arc crust. Geological Society of America, Bulletin, 103: 37～47.

Deckart K, Silva W, Spr ? hnle C, Vela I. 2014. Timing and duration of hydrothermal activity at the Los Bronces porphyry cluster: an update. Mineralium Deposita, 49:535～546.

Dickinson W R, Snyder W S. 1979. Geometry of subducted slabs related to the San Andreas transform. Journal of Geology, 87: 609～627.

Eggins S M. 1993. Origin and differentiation of picritic arc magmas, Ambae (Aoba), Vanuatu. Contributions to Mineralogy and Petrology, 114: 79～100.

Eichelberger J C. 1995. Silicic volcanism: Ascent of viscous magmas from crustal reservoirs. Annual Review of Earth and Planetary Sciences, 23: 41～63.

Fraser R J. 1993. The Lac Troilus Gold-Copper Deposit, Northwestern Quebec: A Possible Archean Porphyry System. Economic Geology, 88: 1685～1699.

Glazner A F. Ussler W. 1988. Trapping of magma at midcrustal density discontinuities. Geophysical Research Letters, 15: 673～675.

Greene A R, Debari S M, Kelemen P B, Blusztajn J, Clift P D. 2006. A detailed geochemical study of island arc crust: The Talkeetna Arc section, south-central Alaska. Journal of Petrology, 47: 1051～1093.

Grove T L, Chatterjee N, Parman S W, Médard E. 2006. The influence of H_2O on mantle wedge melting. Earth and Planetary Science Letters, 249: 74～89.

Grove T L, Till C B, Krawczynski M J. 2012. The role of H_2O in subduction zone magmatism. Annual Review of Earth and Planetary Sciences, 40: 413～439.

Groves D I, Bierlein F P, Meinert L D, Hitzman M W. 2010. Iron oxide copper-gold (IOCG) deposits through Earth history: Implications for origin, lithospheric setting, and distinction from other epigenetic iron oxide deposits. Economic Geology, 105: 641～654.

Gutscher M A, Maury R, Eissen J P, Bourdon E. 2000. Can slab melting be caused by flat subduction?Geology, 28: 535～538.

Hamlyn P R, Keays R R, Cameron W E, Crawford AJ, Waldron H M. 1985. Precious metals in magnesian low-Ti lavas: Implication for metallogenesis and sulfur saturation in primary magmas. Geochimica et Cosmochimica Acta, 49: 1797～811.

Haschke M, Ahmadian J, Murata M, McDonald I. 2010. Copper mineralization prevented by arc-root delamination during Apline-Himalayan collision in Iran. Economic Geology, 105: 855～865.

Hassanzadeh J. 1993. Metallogenic and tectono-magmatic events in the SE sector of the Cenozoic active continental margin of Iran (Shahr e Babak area, Kerman province). Unpublished Ph. D. thesis, University of California, Los Angeles, 204.

Hedenquist J W, Lowenstern J B. 1994. The role of magmas in the formation of hydrothermal ore-deposits. Nature, 370(6490): 519～527.

Heinrich C A, Neubauer F. 2002. Cu-Au-Pb-Zn-Ag metallogeny of the Alpine-Balkan-Carpathian-Dinaride geodynamic province. Mineralium Deposita, 37: 533～540.

Heithersay P S, Walshe J L. 1995. Endeavour 26 North: A Porphyry Copper-Gold Deposit in the Late Ordovician, Shoshonitic Goonumbla Volcanic Complex, New South Wales, Australia. Economic Geology, 90: 1506～1532

Herzberg C T, Fyfe W S, Carr M J. 1983. Density constraints on the formation of the continental Moho and crust. Contributions to Mineralogy and Petrology, 84: 1～5.

Hezarkhani A. 2006. Hydrothermal evolution of the Sar-Cheshmeh porphyry Cu-Mo deposit, Iran: Evidence from fluid inclusions. Journal of Asian Earth Sciences, 28: 409～422

Hildreth W, Moorbath S. 1988. Crustal contributions to arc magmatism in the Andes of central Chile. Contributions to Mineralogy and Petrology, 98: 455～489.

Hollings P, Sweet G, Baker M, Cooke D R, Friedman R. 2013. Tectomegmatic controls on porphyry mineralization: Geochemical evidence from the Black Mountain porphyry system, Philippines. In: eds. Colpron, M., Bissig, T., Rusk, B. G., Thompson, J. F. H., Tectonics, Metallogeny, and Discovery: The North American Cordillera and Similar Accretionary Settings. Society of Economic Geologists, Inc. Special Publication, 17: 301～335.

Hollister V F, Potter R R, Barker A L. 1974. Porphyry-type deposits of the Appalachian Orogen. Economic Geology, 69: 618～630.

Hou Z Q, Gao Y F, Qu X M, Rui Z Y, Mo X X. 2004. Origin of adakitic intrusives generated during mid-Miocene east-west extension in southern Tibet. Earth Planet Science Letter, 220: 139～155

Hou Z Q, Qu X M, Wang S X, Gao Y F, Du A D, Huang W. 2003. Re-Os age for molybdenite from the Gangdese porphyry copper belt on Tibetan plateau: implication for geodynamic setting and duration of the Cu mineralization. Science in China (Series D), 33, 509～618.

Hou Z Q, Yang Z M, Qu X M, Meng X J, Li Z Q, Beaudoin G, Rui, Z Y, Gao Y F. 2009. The Miocene Gangdese porphyry copper beltgenerated during post-collisional extension in the Tibetan Orogen. Ore Geology Reviews, 36: 25～51

Hou Z Q, Zhang H R, Pan X F, Yang, Z M. 2011. Porphyry Cu (Mo-Au) systems in non-arc settings: Examples from the Tibetan-Himalyan orogens and the Yangtze block. Ore Geology Reviews, 39: 21～45.

Hou Z Q, Zhen Y C, Yang Z M, Rui Z Y, Zhao Z D, Jiang S H, Qu X M, Sun Q Z. 2013. Contribution of mantle components within juvenile lower-crust to collisional zone porphyry Cu systems in Tibet. Mineralium Deposita, 48: 173～192

Huppert H E, Woods A W. 2002. The role of volatiles in magma chamber dynamics. Nature, 420: 493～495.

Ivanhoe Mines, 2004. The Oyu Tolgoi copper and gold deposits, south Gobi, Mongolia. University of Tasmania, Centre for Ore Deposit Research Special Publication, 5: 35～40.

James D, Sacks I S. 1999. Cenozoic formation of the central Andes: A geophysical perspective: Society of Economic Geologists, Inc. Special Publication, 7: 1～25.

Jaupart C, Allègre C J. 1991. Gas content, eruption rate and instabilities of eruption regime in silicic volcanoes. Earth and Planetary Science Letters, 102: 413～429.

Jégo S, Pichavant M. 2012. Gold solubility in arc magmas: Experimental determination of the effect of sulfur at 1000°C and 0.4 GPa. Geochimica et Cosmochimica Acta, 84: 560～592.

Jenner F E, O'Neill H S C, Arculus R J, Mavrogenes J A. 2010. The magnetite crisis in the evolution of arc-related magmas and the initial concentration of Au, Ag and Cu. Journal of Petrology, 51: 2445～2464.

Jones G J. 1985. The Goonumbla Porphyry Copper Deposits, New South Wales. Economic Geology, 80: 591～613.

Jugo P J, Luth R W, Richards J P. 2005. An experimental study of the sulfur content in basaltic melts saturated with immiscible sulfide or sulfate liquids at 1300°C and 1.0 GPa. Journal of Petrology, 46: 783～798.

Jugo P J, Wilke M, Botcharnikov R E. 2010. Sulfur K-edge XANES analysis of natural and synthetic basaltic glasses: Implications for S speciation and S content as function of oxygen fugacity. Geochimica et Cosmochimica Acta, 74: 5926～5938.

Kelley K A, Plank T, Newman S, Stolper E M, Grove T L, Parman S, Hauri E. 2010. Mantle melting as a function of water content beneath the Mariana Arc. Journal of Petrology, 51: 1711～1738.

Kerrich R, Goldfarb R, Groves D, Garwin S. 2000. The geodynamics of world-class gold deposits: Characteristics, space-time distributions, and origins. Reviews in Economic Geology, 13: 501～551.

Kirkham R V, Dunne K P E. 2000. World distribution of porphyry, porphyry-associated skarn, and bulk-tonnage epithermal deposits and occurrences. Geological Survey of Canada Open File, 3792a, 26 p.

Klemm L M, Pettke T, Heinrich C A. 2008. Fluid and source magma evolution of the Questa porphyry Mo deposit, New Mexico, USA. Mineralium Deposita, 43: 533～552.

Klepeis K A, Clarke G L, Rushmer T. 2003. Magma transport and coupling between deformation and magmatism in the continental lithosphere. GSA Today, 13: 4～11.

Lang J, Gregory M J, Rebagliati C M, Payne J G, Oliver J L, Roberts K. 2013. Geology and magmatic-hydrothermal evolution of the Giant Pebble porphyry copper-gold-molybdenum deposit, Southwest Alaska. Economic Geology, 108: 437～462.

Leveille R A, Stegen R J. 2012. The Southwestern North America porphyry copper province. In eds. Hedenquist, J. W., Harris, M., and Camus, F., Geology and genesis of the major copper deposits and districts of the World: A Tribute to Richard H. Sillitoe. Society of Economic Geologists, 16: 361～401.

Li J X, Qin K Z, Li G M, Xiao B, Zhao J X, Chen L. 2011. Magmatic-hydrothermal evolution of the Cretaceous Duolong gold-rich porphyry copper deposit in the Bangongco metallogenic belt, Tibet: Evidence from U-Pb and $^{40}Ar/^{39}Ar$ geochronology. Journal of Asia Earth Sciences, 41(6): 525～536.

Ling M X, Wang F Y, Ding X, Hu, Y H, Zhou J B, Zartman R E, Yang X Y, Sun W D. 2009. Cretaceous ridge subduction along the Lower Yangtze River Belt, eastern China. Economic Geology, 104: 303～321.

Lipman P W. 2007. Incremental assembly and prolonged consolidation of cordilleran magma chambers: Evidence from the Southern Rocky Mountain volcanic field. Geosphere, 3: 42～70.

Liu B, Liu H, Zhang C Q, Mao Z, Zhou Y M, Huang H, Su G S. 2014. Geochemistry and geochronology of porphyries from Beiya gold polymetallic deposit, western Yunnan, China. Ore Geology Reviews (in revision).

Liu X, Fan H R, Santosh M, Hu F F, Yang K F, Li Q L, Yang Y H, Liu Y S. 2012. Remelting of Neoproterozoic relict volcanic arcs in the Middle Jurassic: implication for the formation of the Dexing porphyry copper deposit, Southeastern China. Lithos, 150: 85～100.

Livingston D E. 1973. A plate tectonic hypothesis for the genesis of porphyry copper deposits of the southern Basin and Range province. Earth and Planetary Science Letters, 20: 171～179.

Lowell J D. 1974. Regional characteristics of porphyry copper deposits of the Southwest. Economic Geology, 69: 601～617.

Lowell J D, Guilbert J M. 1970. Lateral and vertical alteration-mineralization zoning in porphyry ore deposits. Economic Geology, 65: 373～408.

Lu Y J, Kerrich R, Kemp A I S, McCuaig C T, Hou Z Q, Hart C J R, Li Z X, Cawood P A, Bagas L, Yang Z M, Cliff J, Belousova E A, Jourdan F, Evans N J. 2013. Intracontinental Eocene-Oligocene Porphyry Cu Mineral Systems of Yunnan, Western Yangtze Craton, China: Compositional Characteristics, Sources, and Implications for Continental Collision Metallogeny. Economic Geology, 108: 1541～1576.

Mahdavi A, Karimpour M H, Mao J W, Haidarian Shahri M R, Malekzadeh Shafaroudi A. 2015. Porphyry Copper deposits of Iran: spatial-temporal distribution and their geodynamic settings. Ore Geology Reviews, (preparation to be submitted).

Mao J W, Pirajno F, Lehmann B, Luo M C, Berzina A. 2014. Distribution of porphyry deposits in the Eurasian continent and their corresponding tectonic settings. Journal of Asian Earth Sciences, 79: 576～584.

Mao J W, Cheng Y B, Chen M H, Pirajno F. 2013. Major types and time-space distribution of Mesozoic ore deposits in South China and their geodynamic settings. Mineralium Deposita, 48: 267～294.

Mao J W, Pirajno F, Cook N. 2011a. Mesozoic metallogeny in East China and corresponding geodynamic settings: an introduction to the special issue. Ore Geology Reviews, 43: 1～7.

Mao J W, Xie G Q, Duan C, Pirajno F, Ishiyama D, Chen Y C, 2011b. A tectonogenetic model for porphyry-skarn-stratabound Cu-Au-Mo-Fe and magnetite-apatite deposits along the Middle-Lower Yangtze River Valley, Eastern China. Ore Geology Reviews, 43: 294～314.

Mao J W, Zhang J D, Pirajno F, Ishiyama D, Su H M, Guo C L, Chen Y C. 2011c. Porphyry Cu-Au-Mo—epithermal Ag-Pb-Zn—distal hydrothermal Au deposits in the Dexing area, Jiangxi province, East China; a linked ore system. Ore Geology Reviews, 43: 203～216.

Mao J W, Pirajno F, Xiang J F, Gao J J, Ye H S, Li Y F, Guo B J. 2011d. Mesozoic molybdenum deposits in the East Qinling-Dabie Orogenic belt: characteristics and tectonic settings. Ore Geology Reviews, 43: 264～293.

Mao J W, Wang Y T, Lehmann B, Yu J J, Du A D, Mei Y X, Li Y F, Zang W S, Stein H J., Zhou T F. 2006. Molybdenite Re-Os and albite $^{40}Ar/^{39}Ar$ dating of Cu-Au-Mo and magnetite porphyry systems in the Changjiang valley and metallogenic implications. Ore Geology Reviews, 29: 307～324.

Mao J W, Xie G Q, Bierlein F, Ye H S, Qü W J, Du A D, Pirajno F, Li H M, Guo B J, Li Y F, Yang Z Q. 2008. Tectonic implications from Re-Os dating of Mesozoic molybdenum deposits in the East Qinling-Dabie orogenic belt. Geochimica et Cosmochimica Acta, 72: 4607～4626.

Mao J W, Goldfarb R J, Zhang Z W, Xu W Y, Qiu Y M, Deng J. 2002. Gold deposits in the Xiaoqinling-Xiong'ershan region, Qinling Mountains, central China. Mineralium Deposita, 37: 306～325.

McInnes B I A, Evans N J, Belousova E, Griffin W T, Andrew R L. 2003. Timing of mineralization and exhumation processes at the Sar Cheshmeh and Meiduk porphyry Cu deposits, Kerman belt, Iran, in Eliopouloset al., eds., Mineral exploration and sustainable development: Rotterdam, Millpress, 1197～1200.

McInnes B I A, Evans N J, Fu F Q, Garwin S, Belousova E, Griffin W L, Bertens A, Sukama D, Permanadewi S, Andrew R L, Deckart K. 2005. Thermal history analysis of selected Chilean, Indonesian, and Iranian porphyry Cu-Mo-Au deposits. In: Porter T M. (Ed.), Supper porphyry copper and gold deposits: A global perspective. PGC publishing, Adelaide, 1～16.

Mirnejad H, Mathur R, Hassanzadeh J, Shafie B, Nourail S. 2013. Linking Cu mineralization to host porphyry emplacement: Re-Os ages of molybdenites versus U-Pb ages of zircons and sulfur isotope compositions of pyrite and chalcopyrite from the Iju and Sarkuh porphyry deposits in Southeast Iran. Economic Geology, 108: 861～870.

Mohajjel M, Fergusson C L, Sahandi M R. 2003. Cretaceous-Tertiary convergence and continental collision, Sanandaj-Sirjan zone, western Iran. Journal of Asian Earth Sciences, 21: 397～412.

Moore G M, Carmichael I S E. 1998. The hydrous phase equilibria (to 3 kbar) of an andesite and basaltic andesite from western Mexico: Constraints on water content and conditions of phenocryst growth. Contributions to Mineralogy and Petrology, 130: 304～319.

Mueller D, Groves D I. 2000. Potassic igneous rocks and associated gold-copper mineralization (3rd edition). Berlin: Springer, 252 p.

Murphy J B. 2001. Flat slab subduction in the geological record: Consideration of modern analogues (abs.). Geological Society of America Abstracts with Programs, 33(6): 208.

Naney M T. 1983. Phase equilibria of rock-forming ferromagnesian silicates in granite systems. American Journal of Science, 283: 993～1033.

Oyarzun R, Márquez A, Lillo J, López I, Rivera S. 2001. Giant versus small porphyry copper deposits of Cenozoic age in northern Chile: adakitic versus normal cal-alkaline magmatism. Mineralium Deposita, 36:794～798.

Parkinson I J, Arculus R J. 1999. The redox state of subduction zones: Insights from arc-peridotites. Chemical Geology, 160: 409～423.

Peacock S M. 1993. Large-scale hydration of the lithosphere above subducting slabs. Chemical Geology, 108: 49～59.

Perkins C, Mcdougall I, Claoue-Long J, Hiethersay P S. 1990. $^{40}Ar/^{39}Ar$ and U-Pb geochronology of the Goonumbla porphyry Cu-Au deposits, New South Wales, Australia. Economic Geology, 85: 1808～1824.

Pettke T, Oberli F, Heinrich C A. 2010. The magma and metal source of giant porphyry-type ore deposits, based on lead isotope microanalysis of individual fluid inclusions. Earth and Planetary Science Letters, 296: 267～277.

Pichavant M, Mysen B O, Macdonald R. 2002. Source and H_2O content of high-MgO magmas in island arc settings: An experimental study of a primitive calc-alkaline basalt from St. Vincent, Lesser Antilles arc. Geochimica et Cosmochimica Acta, 66: 2193～2209.

Pollard P J, Taylor R G, Peter L. 2005. Ages of intrusion, alteration, and mineralization at the Grasberg Cu-Au deposit, Papua, Indonesia. Economic Geology, 100: 1005～1020.

Qin K Z. 2011. Thematic Articles "Porphyry Cu-Au-Mo deposits in Tibet and Kazakhstan". Resource Geology, 62(1): 1～3.

Qu X M, Hou Z Q, Li Y G. 2004. Melt components derived from a subducted slab in late orogenic ore-bearing porphyries in the Gangdese copper belt, southern Tibetan plateau. Lithos, 74: 131～148.

Qu X M, Hou Z Q, Zaw K, Li Y G. 2007. Characteristics and genesis of Gangdese porphyry copper deposits in the southern Tibetan Plateau: preliminary geochemical and geochronological results. Ore Geology Reviews, 31: 205～223.

Richards J P 1995. Alkalic-type epithermal gold deposits: A review. In: Thompson J F H, ed., Magmas, fluids, and ore deposits: Mineralogical Association of Canada Short Course Series, 23: 367～400.

Richards J P. 2003, Tectono-magmatic precursors for porphyry Cu-(Mo-Au) deposit formation. Economic Geology, 96: 1515～1533.

Richards J P. 2013. Giant ore deposits formed by optimal alignments and combinations of geological processes. Nature Geoscience, 6 (11): 911～916.

Richards J P, Chappell B W, McCulloch M T. 1990. Intraplate-type magmatism in a continent-island-arc collision zone: Porgera intrusive complex, Papua New Guinea. Geology, 18: 958～961.

Richards S W, Holm R J. 2013. Tectonic preconditioning and the Formation of Giant porphyry deposits. In: Colpron M, Bissig T, Rusk B G, Thompson J F H, eds. Tectonics, Metallogeny, and Discovery: The North American Cordillera and Similar Accretionary Settings. Society of Economic Geologists, Inc. Special Publication, 17: 265～275.

Rutherford M J, Devine J D. 1988. The May 18, 1980, eruption of Mount St. Helens. 3 Stability and chemistry of amphibole in the magma chamber. Journal of Geophysical Research, 93 (11): 959949～11.

Schmidt M W, Poli S. 1998. Experimentally based water budgets for dehydrating slabs and consequences for arc magma generation. Earth and Planetary Science Letters, 163: 361～379.

Seltmann R, Porter T M, Pirajno F. 2014. Geodynamics and metallogeny of the central Eurasian porphyry and related epithermal mineral systems: a review. Journal of Asian Earth Sciences, 79 (Part B): 810～841.

Shafiei B, Haschke M, Shahabpour J. 2009. Recycling of orogenic arc crust triggers porphyry Cu mineralization in Kerman Cenozoic arc rocks, southeastern Iran. Mineralium Deposita, 44: 265～283.

Sikka D B, Nehru C E. 1997. Review of porphyry Cu ± Mo ± Au deposits with special references to Malajkh porphyry copper deposit, Madhya Pradesh. Journal of Geological Society of India, 49: 239～288.

Sillitoe R. 1997. Characteristics and controls of the largest porphyry copper-gold and epithermal gold deposits in the circum-Pacific region. Australian Journal of Earth Sciences, 44: 373～388.

Sillitoe R. 1998, Major regional factors favoring large size, high hypogene grade, elevated gold content and supergene oxidation and enrichment of porphyry copper deposits. In Porter T M, ed. Porphyry and hydrothermal copper and gold deposits: A Global Perspective, Perth, 1998, Conference Proceedings: Glenside, South Australia, Australian Mineral Foundation, 21～34.

Sillitoe R. 2012. Copper province. In: Hedenquist J W, Harris M, and Camus F eds. Geology and Genesis of the Major Copper Deposits and Districts of the World: A Tribute to Richard H. Sillitoe. Society of Economic Geologists, 16: 1～18.

Sillitoe R. 2013. Metallogenic and regulatory inequalities around the Northern Pacific Rim: Implications for discovery. Society of Economic Geologists, Inc. Special Publication, 17: 1～16.

Sillittoe R. 1972. A plate tectonic model for the origin of porphyry copper deposits. Economic Geology, 67: 184～197.

Sobolev A, Chaussidon M. 1996. H_2O concentrations in primary melts from supra-subduction zones and mid-ocean ridges: Implications for H_2O storage and recycling in the mantle. Earth and Planetary Science Letters, 137: 45～55.

Sun J, Mao J, Beaudoin G, Yao F, Yuan S, Li T, Duan X, Wu Y. 2014. Geological evolution of magmatism and mineralization in the Duolong region, northwestern Tibet, China: Constraints from U-Pb, Re-Os, $^{40}Ar/^{39}Ar$ data and Hf isotopes. Mineralium Deposita (Submitted).

Sun W D, Huang R F, Li H, Hu Y B, Zhang C C, Sun S J, Zhang L P, Ding X, Li C Y, Zartman R E, Ling M X. 2014. Porphyry deposits and oxidized magmas. Ore Geology Reviews, 65: 97～131.

Sun W D, Ling M X, Yang X Y, Fan W M, Ding X, Liang H Y. 2010. Ridge subduction and porphyry copper-gold mineralization: an overview. Science in China Series D Earth

Science, 53(4): 475～484.

Tafti R, Mortensen J K, Lang J R, Rebaglitim M, Oliver J L. 2009. Jurassic U-Pb and Re-Os ages for the newly discovered Xietongmen Cu-Au porphyry district, Tibet, PRC: implications for metallogenic epochs in the southern Gangdese belt. Economic Geology, 104, 127～136.

Taghipour N, Aftabi A, Mathur R. 2008. Geology and Re-Os geochronology of mineralization of the Miduk porphyry copper deposit, Iran. Resource Geology, 58: 143～160.

Tatsumi Y. 1986. Formation of the volcanic front in subduction zones. Geophysical Research Letters, 17: 717～720.

Tatsumi Y. 1989. Migration of fluid phases and genesis of basalt magmas in subduction zones: Journal of Geophysical Research, 94: 4697～4707.

Thirlwall M F, Graham A M, Arculus R J, Harmon R S, Macpherson C G. 1996. Resolution of the effects of crustal assimilation, sediment subduction, and fluid transport in island arc magmas: Pb-Sr-Nd-O isotope geochemistry of Grenada, Lesser Antilles. Geochimica et Cosmochimica Acta, 60: 4785～4810.

Thorkelson D J. 1996. Subduction of diverging plates and the principles of slab window formation. Tectonophysics, 255(1～2): 47～63.

Titley S R, Beane R E. 1981. Porphyry copper deposits; Part I. Geologic settings, petrology, and tectogenesis. Economic Geology's 75th Anniversary Volume, 214～234.

Titley S R. 1993. Characteristics of porphyry copper occurrence in the American Southwest. In: Kirkham R V, Sinclair W D, Thorpe R I, and Duke J M, eds. Mineral exploration modeling. Geological Association of Canada Special Paper, 40: 433～464.

Tran M D, Liu J L, Nguyen Q L, Chen Y, Tang Y, Song Z J, Zhang Z C, Zhao Z D. 2014. Cenozoic high-K alkaline magmatism and associated Cu-Mo-Au mineralization in the Jinping-Fan Si Pan region, southeastern Ailao Shan-Red River shear zone, southwestern China-northwestern Vietnam. Journal of Asian Earth Sciences, 79 (Part B): 858～872.

Ulmer P. 2001. Partial melting in the mantle wedge—The role of H_2O in the genesis of mantle-derived "arc-related" magmas. Physics of the Earth and Planetary Interiors, 127: 215～232.

Uyeda S, Miyashiro A. 1974. Plate tectonics and the Japanese island: A synthesis. Geological Society of America Bulletin, 85: 1159～1170.

Walker G. P L. 1989. Gravitational (density) controls on volcanism, magma chambers and intrusions. Australian Journal of Earth Sciences, 36: 149～165.

Wallace P J. 2005. Volatiles in subduction zone magmas: Concentrations and fluxes based on melt inclusion and volcanic gas data. Journal of Volcanology and Geothermal Research, 140: 217～240.

Wallace P J, Edmonds M. 2011. The sulfur budget in magmas: evidence from melt inclusions, submarine glasses, and volcanic gas emissions. Reviews in Mineralogy and Geochemistry, 73: 215～246.

Wang R, Richards J P, Hou Z Q, Yang Z M. 2014. Extent of underthrusting of the Indian plate beneath Tibet controlled the distribution of Miocene porphyry Cu-Mo ± Au deposits. Mineralium Deposita, 49: 165～173.

Wilkinson J J. 2013. Triggers for the formation of porphyry ore deposits in magmatic arcs. Nature Geoscience, 6 (11): 917～925.

Wilson A, Cooke D R, Stein H J, Fanning M C, Holliday J, Tedder I J. 2007. U-Pb and Re-Os Geochronologic Evidence for Two Alkalic Porphyry Ore-Forming Events in the Cadia District, New South Wales, Australia. Economic Geology, 102: 3～26.

Xu L L, Bi X W, Hu R Z, Tang Y Y, Jiang G H, Qi Y Q. 2014. Origin of the ore-forming fluids of the Tongchang porphyry Cu-Mo deposit in the Jinshajiang-Red River alkaline igneous belt, SW China: constraints from He, Ar and S isotopes. Journal of Asian Earth Sciences, 79 (Part B): 884～894.

Yakubchuk A, Degtyarev K, Maslennikov V, Wurst A, Stekhin A, Lobanov K. 2012. Tectonomagmatic settings, architecture, and metallogeny of the Central Asian copper province. In eds. Hedenquist, J. W., Harris, M., and Camus, F., Geology and Genesis of the Major Copper Deposits and Districts of the World: A Tribute to Richard H. Sillitoe. Society of Economic Geologists, 16: 403～432.

Yang Z M, Hou Z Q, Xu J F, Bian X F, Wang G R, Yang Z S, Tan S H, Liu Y C, Wang ZL. 2014. Geology and origin of the post-collisional Narigongma porphyry Cu-Mo deposit, southern Qinghai, Tibet. Gondwana Research, 26: 536～556.

Yigit O. 2009. Mineral Deposits of Turkey in Relation to Tethyan Metallogeny: Implications for Future Mineral Exploration. Economic Geology, 104: 19～51.

Zajacz Z, Halter W E, Pettke T, Guillong M. 2008. Determination of fluid/melt partition coefficients by LA-ICPMS analysis of co-existing fluid and silicate melt inclusions: controls on element partitioning. Geochimica et Cosmochimica Acta, 72: 2169～2197.

Zheng Y Y, Sun X, Gao S B, Zhao Z D, Zhang G Y, Wu S, You Z M, Li J D. 2014. Multiple mineralization events at the Jiru porphyry copper deposit, southern Tibet: implications for Eocene and Miocene magma sources and resource potential. Journal of Asian Earth Sciences, 79 (Part B): 842～857.

Zhou T F, Wang S W, Fan Y, Yuan F, Zhang D Y, White N C. 2014. A review of the intracontinental porphyry deposits in the Middle-Lower Yangtze River Valley metallogenic belt, Eastern China. Ore Geology Reviews, DOI: doi: 10.1016/j.oregeorev.2014.10.002.

Zimmer M M, Plank T, Hauri E H, Yogodzinski G M, Stelling P, Larsen J, Singer B, Jicha B. Mandeville C, Nye C J. 2010. The role of water in generating the calc-alkaline trend: New volatile data for Aleutian magmas and a new Tholeiitic Index. Journal of Petrology, 51: 2411～2444.

Basic Characteristics and New Advances in Research and Exploration on Porphyry Copper Deposits

MAO Jingwen[1), LUO Maocheng[2), XIE Guiqing[1), LIU Jun[1), WU Shenghua[1)

1) *MLR Key Laboratory of Metallogeny and Mineral Assessment, Institute of Mineral Resources, Chinese Academy of Geological Sciences, Beijing*, 100037; 2) *School of Earth Sciences and Resources, China University of Geosciences, Beijing*, 100083

Abstract

Porphyry Cu deposits, constituting the world's major source of Cu, have been major research and exploration target for a long time. Since the new century, not only mineral exploration but researches have made significant progress. So far proven porphyry Cu metal reserves in the world are 1.8 billion tons, and mainly distributed in the western continental margins of North and South America, South-west Pacific Island arc, Central Asian countries, and Tethyan belt (mainly comprising Eastern Europe segment, Iran-Pakistan segment, Tibetan areas in China), of which the western continental margins of South America contain 1.1 billion tons of Cu metal reserve. Proven porphyry Cu ore reserves explored increase through the geological history from the Precambrian, Early Paleozoic, Late Paleozoic, and Mesozoic to Cenozoic. Porphyry Cu deposits predominantly are located in suprasubduction zone where the porphyry Cu-Au deposits formed in island arc, and porphyry Cu-Mo or Cu-Mo($\pm$Au) deposits formed in continental margin. The subduction angle variation of slab from steep to gentle, even flat, is responsible for the formation of the porphyry Cu deposits; formation of giant deposits is spatially associated with the flat slab subduction of aseismic ridges, seamounts and oceanic plateau. The transform faults within oceanic plates are easily replaced by seawater, of which these subducted faults beneath continent or island arc are favorable for the formation of ore-forming magma; and the conjunction belts of varied tectonic units in the continents, where subducted slabs are susceptible to tear up, is also an important place of forming porphyry Cu system. The partial melting of the asthenosphere mantle wedge, which had undergone metasomatism induced by the subduction fluid, has been considered to be main forming process of the arc magma, since the subducted slab carries abundant seawater and seafloor sediments (comprising sulfates) into the asthenosphere. The basic magma with high oxidation extent and rich volatile experienced the MASH and differentiation process in the lower crust, gradually evolved into intermediate-acidic ore-forming magma with light specific weight. The magmas ascend to the shallow position along fault zones and finally formed deposits. The studies of continental porphyry Cu deposits has been paid more attention in the last 10 years. The arguement is that the ore-forming materials are derived from the crust-mantle interaction of continental interiors (include juvenile lower crust) or the metasomatic lithosphere originated from remelting of residual subducted slab. The studies of deposit models from the single mineralized alteration model to the deposit model of a group of minerals with genetic relationship are more importance for the perspective of mineral exploration. In addition, the research of the Footprint with altered minerals of porphyry Cu deposits system (e.g. chlorite, epidote, alunite and clay minerals), has been paid more attentions and used for the prospecting and exploration.

Key words: porphyry Cu deposit; subduction and mineralization; continental mineralization; temporal-spatial distribution; deposit model